© 2016. Published by The Company of Biologists Ltd | Development (2016) 143, 1363-1374 doi:10.1242/dev.132159

RESEARCH ARTICLE

A direct role for murine Cdx proteins in the trunk neural crest gene regulatory network

Oraly Sanchez-Ferras*,‡, Guillaume Bernas‡, Omar Farnos, Aboubacrine M. Touré, Ouliana Souchkova and Nicolas Pilon§

ABSTRACT

Numerous studies in chordates and arthropods currently indicate that Cdx proteins have a major ancestral role in the organization of post-head tissues. In urochordate embryos, Cdx loss-of-function has been shown to impair axial elongation, neural tube (NT) closure and pigment cell development. Intriguingly, in contrast to axial elongation and NT closure, a Cdx role in neural crest (NC)-derived melanocyte/pigment cell development has not been reported in any other chordate species. To address this, we generated a new conditional pan-Cdx functional knockdown mouse model that circumvents Cdx functional redundancy as well as the early embryonic lethality of Cdx mutants. Through directed inhibition in the neuroectoderm, we provide *in vivo* evidence that murine Cdx proteins impact melanocyte and enteric nervous system development by, at least in part, directly controlling the expression of the key early regulators of NC ontogenesis *Pax3*, *Msx1* and *Foxd3*. Our work thus reveals a novel role for Cdx proteins at the top of the trunk NC gene regulatory network in the mouse, which appears to have been inherited from their ancestral ortholog.

KEY WORDS: Cdx, Neural crest, Gene regulatory network, Melanocyte, Peripheral nervous system, Enteric nervous system

INTRODUCTION

The neural crest (NC) is a vertebrate-specific population of multipotent cells that arise at a precise region of the embryo called the neural plate border (between the neural and non-neural ectoderm). Rolling-up of the neural plate during neurulation places the recently induced NC cells (NCCs) in the dorsal part of the closing neural tube (NT), from where they emigrate to colonize the embryo and differentiate into many derivatives (Bronner and LeDouarin, 2012). According to their location along the anterior-posterior (A-P) axis, pre-migratory NCCs are classified into cranial, cardiac, vagal, trunk and sacral populations. The trunk NCC population has the unique potential to migrate either ventrally through the somites to give rise to neural derivatives (such as neurons and glia of the dorsal root and sympathetic ganglia), or dorsolaterally beneath the surface ectoderm to give rise to melanocytes of the skin (Kuo and Erickson, 2010). The melanin-producing melanocytes appear to represent the most ancient evolutionarily conserved NC-like derivative (Abitua et al., 2012; Jeffery et al., 2008).

Evidence from the study of the cranial NC population in zebrafish, chick and frog embryos has led to a putative NC gene regulatory network (GRN) (Simoes-Costa and Bronner, 2015; Stuhlmiller and García-Castro, 2012). This network notably involves the convergence of posteriorizing (canonical Wnt and FGF) and mediolateral (BMP) signaling inputs at the neural plate border and the stepwise induction of, first, a kernel of 'neural plate border specifier' genes that encode transcription factors such as Pax3/7, Msx1/2 and Zic1/2, followed by a second module of 'NC specifier' genes that encode transcription factors such as FoxD3 and Sox9/10. A third module of 'NCC effector' genes encoding proteins with various functions (e.g. Dct enzyme and Ret transmembrane receptor) is finally activated during the migration of NCCs in order to control their tissue-specific homing and differentiation. Comparative analysis of the cranial NC GRN from basal chordates to vertebrates suggests that many regulatory circuits are conserved across chordates (Green and Bronner, 2013; Simoes-Costa and Bronner, 2013). However, the exact way in which the NC GRN is wired downstream of the signaling inputs is expected to differ between the cranial and trunk regions, and between species (Barriga et al., 2015; Simoes-Costa and Bronner, 2013). How the trunk NC GRN is wired in the mouse is largely unknown.

The Caudal-related homeobox (Cdx) gene family encode homeodomain transcription factors with posterior-restricted expression patterns and key, evolutionarily conserved roles in the general organization of post-head tissues via both Hox-dependent and -independent means (Copf et al., 2004; Faas and Isaacs, 2009; Katsuyama et al., 1999; Savory et al., 2009a; Shimizu et al., 2005; Shinmyo et al., 2005; Young et al., 2009). Owing to the very high conservation of their homeodomain, murine Cdx proteins (Cdx1/2/4) act redundantly in the regulation of their target genes (Savory et al., 2011, 2009b; van den Akker et al., 2002; van Nes et al., 2006; van Rooijen et al., 2012). Cdx proteins also possess an N-terminal transactivation domain and, accordingly, the vast majority of these target genes are positively regulated (Bansal et al., 2006; Beland et al., 2004; Taylor et al., 1997; Verzi et al., 2011). Between E7.5 and E12.5, robust Cdx gene expression is initiated in epiblast cells undergoing gastrulation in the posterior regions of the embryo (i.e. primitive streak and axial stem cell zone of the tailbud). Cdx gene expression then transiently persists in the neuroectoderm, including in pre-migratory NCCs (Coutaud and Pilon, 2013). At the onset of neurulation (E8.5), this is exemplified by a posterior (high) to anterior (low) gradient of transcript and protein distribution in the developing spinal cord, with an anterior limit of expression around the level of the hindbrain/spinal cord boundary set by Cdx1 (Beck et al., 1995; Gamer and Wright,

Molecular Genetics of Development Laboratory, Department of Biological Sciences and BioMed Research Center, University of Quebec at Montreal (UQAM), Montreal H2X 3Y7, Canada.
*Present address: Goodman Cancer Research Centre and Department of Biochemistry, McGill University, Montreal, H3A 1A3, Canada.
‡These authors contributed equally to this work

§Author for correspondence (pilon.nicolas@uqam.ca)

Received 23 October 2015; Accepted 18 February 2016

Development (2016) 143, 1363-1374 doi:10.1242/dev.132159

1993; Gaunt et al., 2003, 2005; Meyer and Gruss, 1993). This anterior limit of expression is not permanent as it regresses caudally concomitantly with axial elongation. By contrast, robust expression is maintained in the tailbud region until E10.5 for *Cdx1/4* and E12.5 for *Cdx2*. In accordance with their posterior-restricted expression patterns, expression of Cdx genes is regulated by posteriorizing signals (Lohnes, 2003), with all three murine Cdx genes being direct targets of the canonical Wnt pathway (Lickert et al., 2000; Pilon et al., 2006, 2007; Prinos et al., 2001; Zhao et al., 2014).

Pertaining to NC ontogenesis, we previously demonstrated that Cdx proteins act downstream of canonical Wnt signaling to directly induce *Pax3* expression in pre-migratory NCCs in cooperation with the neural plate border specifier Zic2 and the pan-neural factor Sox2 (Sanchez-Ferras et al., 2014, 2012). However, the importance of this regulation for global trunk NC development *in vivo* was not evaluated owing to complications typically associated with the study of Cdx null compound mutants (i.e. posterior truncation and/or early embryonic lethality) (Savory et al., 2011, 2009b; van Rooijen et al., 2012). Via conditional expression of a previously described dominant-negative Cdx protein (Sanchez-Ferras et al., 2012) in the NT and pre-migratory NCCs, we now show that Cdx proteins play a key early role in the trunk NC GRN, with especially notable implications for subsequent melanocyte development.

RESULTS

Generation and validation of a mouse model allowing conditional pan-Cdx functional knockdown

To study the role of Cdx in NC development *in vivo*, we devised a strategy allowing neuroectoderm-specific pan-Cdx functional knockdown. This approach is based on the Cre/loxP-dependent expression of a FLAG-tagged fusion protein ($_{FLAG}$EnRCdx1) consisting of the repressor domain of *Drosophila* Engrailed (EnR) fused to the Cdx1 homeodomain. Both the efficacy and specificity of EnRCdx1 as a potent repressor of Cdx target genes regulated either by DNA binding-dependent (via Cdx BS) or -independent means [via an interaction with a DNA-binding co-factor such as the Wnt nuclear effector Lef1 (Beland et al., 2004)] have been previously validated (Sanchez-Ferras et al., 2012).

As depicted in Fig. 1, a $_{FLAG}$EnRCdx1-IRES-GFP bicistronic cassette preceded by a floxed PGKpNeo cassette was targeted to the *ROSA26* locus by homologous recombination in embryonic stem cells (ESCs), thereby generating a novel *ROSA26* reporter allele that we named *R26R*^{EnRCdx1}. Standard microinjection of these targeted ESCs into blastocysts yielded three germline transmitting chimeras. Following appropriate breeding, *R26R*$^{EnRCdx1/EnRCdx1}$ animals were recovered at the expected frequency and were healthy and fertile.

To validate the efficacy and specificity of the conditional EnRCdx1 mouse model, we evaluated whether it could be used to affect the well-characterized role of Cdx in A-P vertebral

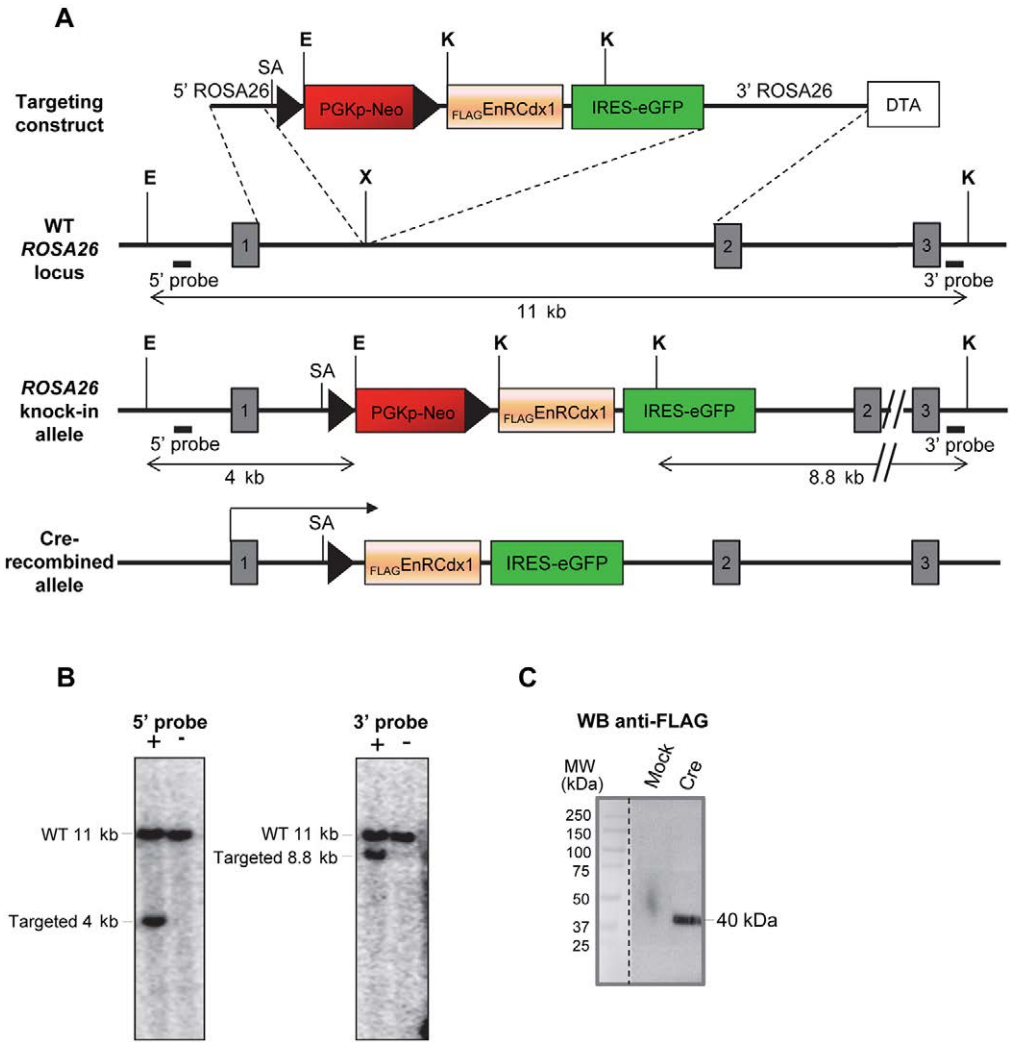

Fig. 1. Targeting of $_{FLAG}$EnRCdx1 coding sequences into the *ROSA26* locus. (A) Targeting strategy showing the insertion of a bicistronic cassette encoding $_{FLAG}$EnRCdx1 and GFP downstream of an intervening floxed PGKpNeo cassette into the *ROSA26* locus. SA, splice acceptor site; E, *Eco*RI; K, *Kpn*I; X, *Xba*I; DTA, diphtheria toxin; WT, wild type. Numbered boxes are exons. (B) Southern blot analysis of *Eco*RI and *Kpn*I double-digested genomic DNA from representative targeted (+) and untargeted (–) ESC clones using the 5′ and 3′ external probes depicted in A. (C) Anti-FLAG western blot confirming expression of $_{FLAG}$EnRCdx1 (~40 kDa) by the injected ESC clone following transfection of Cre-expressing (Cre) or empty (mock) vectors.

Development (2016) 143, 1363-1374 doi:10.1242/dev.132159

patterning (Deschamps and van Nes, 2005; Lohnes, 2003). *R26R*$^{EnRCdx1/EnRCdx1}$ mice were crossed with *T-Cre*$^{Tg/+}$ mice (Perantoni et al., 2005), which express *Cre* in the posterior nascent mesoderm under the control of the brachyury (*T*) promoter (Fig. S1A,B). Skeletal preparations of *R26(TCre)*$^{EnRCdx1/+}$ neonates showed the presence of a high number of homeotic transformations as well as vertebral malformations and/or fusions at the cervical level, most of which were fully penetrant (Fig. 2A, Table 1). Similar defects were also observed in the thoracic and lumbar regions, but with lower penetrance (Fig. 2B-D′). These phenotypes are highly reminiscent of those observed in *Cdx1*$^{-/-}$*; Cdx2*$^{+/-}$ compound mutants (van den Akker et al., 2002). As these defects resulted from only monoallelic expression of EnRCdx1, such an outcome clearly validates the *R26R*^{EnRCdx1} mouse model as a potent genetic tool for conditional Cdx loss-of-function studies.

Pax3 promoter-directed expression of EnRCdx1 results in early postnatal death, hydronephrosis and pigmentation defects

To study Cdx function in the NC lineage, the *P3pro-Cre* driver line was chosen over the widely used *Wnt1-Cre* line in order to avoid the Cdx-free anterior neuroectoderm (Fig. S1C). We reasoned that this would minimize potential off-target effects, which are always a concern with a dominant-negative approach. As previously described (Li et al., 2000; Stottmann and Klingensmith, 2011), analysis of *R26(P3Cre)*$^{EnRCdx1/+}$ E9.5 embryos showed that the *P3pro-Cre* transgene directs expression of the $_{FLAG}$EnRCdx1-IRES-GFP bicistronic cassette in the posterior neural plate up to the posterior hindbrain (Fig. S1D). Of note, still in accordance with prior studies (Liu et al., 2006), transverse sections at the level of the forelimb buds not only revealed strong GFP expression in migratory NCCs but also variable expression throughout the dorsoventral axis of the NT (Fig. S1E).

R26(P3Cre)$^{EnRCdx1/+}$ mutants of weaning age were recovered at lower than expected frequency, and a systematic follow-up of the progeny of six breeding couples revealed that a high number of mutant newborns die at about postnatal day (P) 1 with very little, if any, milk in their stomach (Fig. 3A, Table 2). This age of death, combined with the lack of milk, is normally indicative of severe feeding problems (Turgeon and Meloche, 2009). This is apparently not due to abnormal craniofacial morphology and, as described below, other data rather suggest a neural origin for this outcome (see Fig. 5). Interestingly, about half of *R26(P3Cre)*$^{EnRCdx1/+}$ newborns also exhibit a kinked tail (Fig. 3A, Table 2). This is suggestive of mild convergent extension defects, as previously reported for *Cdx1*$^{+/-}$*;Cdx2*$^{-/-}$ double mutants (Savory et al., 2011), thereby further validating our approach.

Other observations revealed that *R26(P3Cre)*$^{EnRCdx1/+}$ mutants that survive beyond P2 also exhibit severe growth delay (Fig. 3B), with an additional subset of them dying at ∼P10 (Table 2). The cause of this second wave of early postnatal death is currently unclear, although it might well still be due to feeding difficulties. Intriguingly, many of these dead animals exhibited a hydronephrotic kidney upon dissection. However, we think that this phenotype is unlikely to represent a major cause of death given that it was present in only about half of cases, in an age-independent manner, and frequently found to unilaterally affect the left kidney only (Fig. 3C, Table 2). It is also noteworthy that *R26(P3Cre)*$^{EnRCdx1/+}$ mice have reproduction problems that prevented the generation of mutant animals with biallelic expression of EnRCdx1.

Importantly, 100% of *R26(P3Cre)*$^{EnRCdx1/+}$ mice that survive beyond P2 display pigmentation anomalies (Table 2). Lack of pigmentation is observed in the hindpaws and distal tail in all mutants, but never in anterior regions of the body (Fig. 3B). In ∼25% of cases, a tiny white spot is also observed on the belly (Fig. 3D,E). To determine whether these pigmentation defects were specifically caused by reduction in Cdx function, we expressed EnRCdx1 in a *Cdx1*$^{-/-}$ background

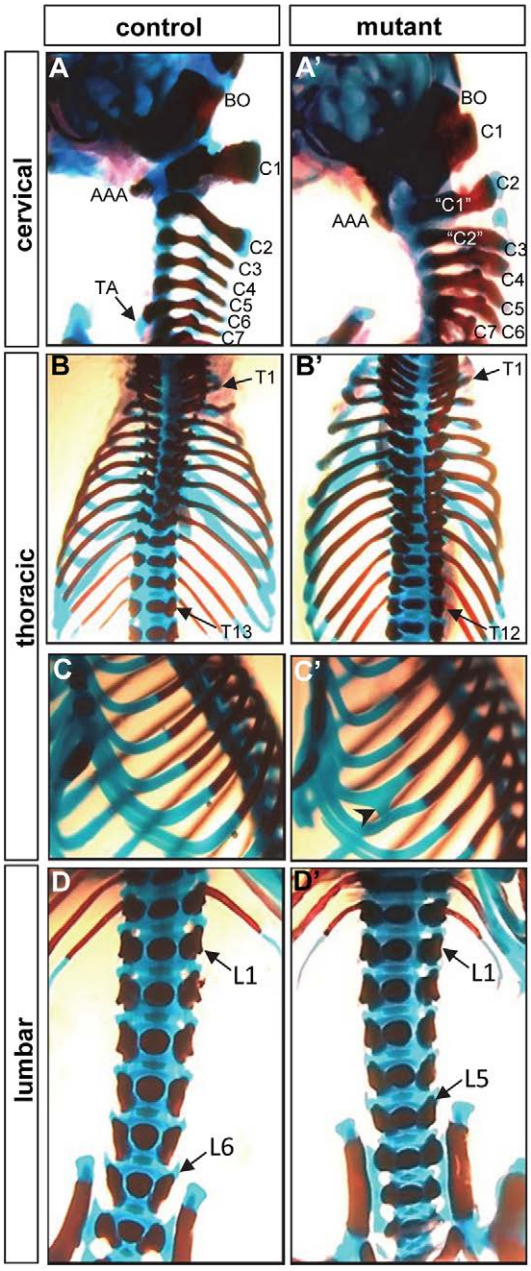

Fig. 2. *T-Cre*-directed expression of $_{FLAG}$EnRCdx1 recapitulates the vertebral A-P patterning defects of Cdx mouse mutants. Representative images of skeletal analyses of *R26R*$^{EnRCdx1/+}$ (control) and *R26(TCre)*$^{EnRCdx1/+}$ (mutant) offspring at P1. (A,A′) Cervical region showing anterior homeotic transformations, malformed neural arches and vertebral fusions in the mutants. Cervical (C) vertebra 1 and associated anterior arch of the atlas (AAA) are fused to the basioccipital (BO) bone, while C2/C3 are anteriorly transformed (denoted C1 and C2) and exhibit malformed neural arches. Note also the absence of the tuberculum anterior (TA) on C6. (B-C′) Thoracic region (B,B′, dorsal view; C,C′, lateral view) showing a reduced number of thoracic (T) vertebrae (12 instead of 13) as well as fusion of ribs (C′, arrowhead) in some mutants. (D,D′) Lumbar region showing that some mutants have only five lumbar (L) vertebrae instead of six.

Development (2016) 143, 1363-1374 doi:10.1242/dev.132159

Table 1. Vertebral phenotypes of *R26(TCre)*$^{EnRCdx1/+}$ mutants

Phenotype	% (number/total)
Cervical region	
Basioccipital	
Fusion to AAA	67 (4/6)
Vertebra 1	
Absence of AAA	17 (1/6)
Fusion to basioccipital	100 (6/6)
Malformed NA	100 (6/6)
Vertebra 2	
C1 identity	100 (6/6)
Fusion to C1	83 (5/6)
Malformed NA	100 (6/6)
Vertebra 3	
C2 identity	67 (4/6)
Fusion to C4	50 (3/6)
Malformed NA	67 (4/6)
Vertebra 4	
Fusion to C3	50 (3/6)
Vertebra 6	
Absence of TA	100 (6/6)
Vertebra 7	
Malformed	17 (1/6)
Thoracic region	
12 thoracic vertebrae instead of 13	17 (1/6)
Fusion of ribs	33 (2/6)
Lumbar region	
5 lumbar vertebrae instead of 6	33 (2/6)

AAA, anterior arch of the atlas; NA, neural arch; TA, tuberculum anterior.

[*R26(P3Cre)*$^{EnRCdx1/+}$::*Cdx1*$^{-/-}$]. Decreasing Cdx dosage significantly increased both the phenotypic penetrance and the extent of white spotting, thereby phenocopying the *Pax3* Splotch heterozygous (*Pax3*$^{Sp/+}$) phenotype in posterior regions (compare Fig. 3E with Fig. 4B,F). Such posterior specificity is in total agreement with the restricted expression of Cdx genes in the posterior embryo and is thus indicative of a new cell-autonomous role for Cdx proteins in trunk NC development.

Genetic interaction between *R26(P3Cre)*$^{EnRCdx1/+}$ and *Pax3*$^{Sp/+}$

Our previous work revealed a key role for Cdx proteins in the induction of *Pax3* expression in trunk NCCs via direct binding to a short evolutionarily conserved enhancer (Sanchez-Ferras et al., 2014, 2012). To expand on this *in vivo*, and based on the presence of *Pax3*$^{Sp/+}$-like pigmentation defects in *R26(P3Cre)*$^{EnRCdx1/+}$ mutants (Fig. 3), we evaluated whether neuroectoderm-directed expression of EnRCdx1 in a *Pax3*$^{Sp/+}$ background would yield a significant reduction in *Pax3* expression to increase the pigmentation defects of *Pax3*$^{Sp/+}$ mice. In accordance with this possibility, phenotypic analyses of an allelic series of *R26R*$^{EnRCdx1/EnRCdx1}$ and *P3pro-Cre*$^{Tg/+}$::*Pax3*$^{Sp/+}$ mice revealed that the posterior pigmentation anomalies observed in each single mutant were significantly accentuated in all double mutants (Fig. 4A-H).

Given the known requirement of *Pax3* function for proper formation of the NC-derived enteric nervous system (Lang et al., 2000), the structure of the myenteric plexus was also analyzed in the distal colon of these mice by staining of acetylcholinesterase activity. Whereas very modest, if any, hypoganglionosis was observed in each single mutant, a clearly aggravated phenotype was again observed in all double mutants tested (Fig. 4I-L). Therefore, these observations strongly suggest that the NC defects observed upon EnRCdx1-mediated Cdx loss-of-function are, at least in part, due to reduced *Pax3* expression.

EnRCdx1-mediated Cdx loss-of-function affects A-P patterning of the peripheral nervous system as well as melanoblast development

The presence of fusions between adjacent NC-derived dorsal root ganglia, which is suggestive of deficient A-P patterning, has previously been described in the cervical region of *Cdx1*$^{-/-}$; *Cdx2*$^{+/-}$ double mutants (van den Akker et al., 2002). To determine whether these defects were cell-autonomous, as well as to obtain an overview of the integrity of the peripheral nervous system upon neural-specific EnRCdx1-mediated Cdx loss-of-function, we stained E10.5 embryos using the 2H3 anti-neurofilament antibody. Comparison between mutant [*R26(P3Cre)*$^{EnRCdx1/+}$::*Cdx1*$^{-/-}$] and control (R26$^{EnRCdx1/+}$::*Cdx1*$^{-/-}$) embryos revealed the presence of fusions of dorsal root ganglia in the cervical region (Fig. 5A-D), thereby indicating a cell-autonomous contribution of Cdx proteins to A-P patterning of NCCs. Interestingly, this analysis also revealed abnormalities of the hypoglossal nerve (twelfth cranial nerve) in mutant embryos. This strictly motor nerve innervates the

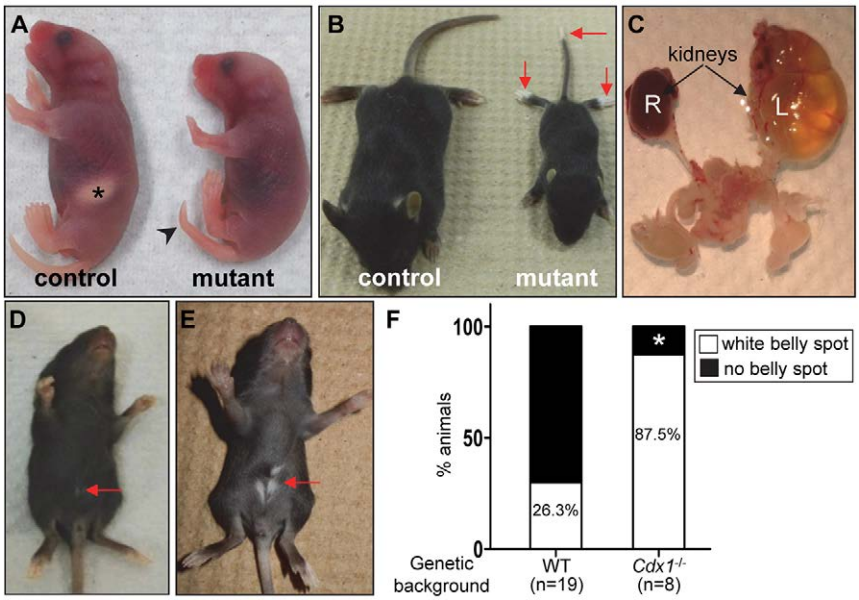

Fig. 3. Overview of phenotypes resulting from *P3pro-Cre*-directed expression of EnRCdx1. (A,B) Comparison between *R26R*$^{EnRCdx1/+}$ (control) and *R26(P3Cre)*$^{EnRCdx1/+}$ (mutant) littermates at P1 (A) and P20 (B). In A, note the absence of the milk spot (asterisk) and the presence of a kinked tail (arrowhead) in the mutant. In B, note the smaller size of the mutant mouse accompanied by depigmentation of the tip of the tail and hindpaws (arrows). (C) Urogenital system of a P90 *R26(P3Cre)*$^{EnRCdx1/+}$ mouse. The left kidney (L) is severely hydronephrotic, whereas the right kidney (R) appears normal. (D,E) P21 mutant mice showing a tiny white belly spot in a *R26(P3Cre)*$^{EnRCdx1/+}$ mutant (D, arrow) and a larger white belly spot in a *R26(P3Cre)*$^{EnRCdx1/+}$::*Cdx1*$^{-/-}$ double mutant (E, arrow). (F) Quantification data showing that the presence of an EnRCdx1-induced white belly spot is dependent on Cdx dosage. The single *R26(P3Cre)*$^{EnRCdx1/+}$::*Cdx1*$^{-/-}$ animal without a white belly spot (asterisk) was also the only one with agouti instead of black coat color.

Development (2016) 143, 1363-1374 doi:10.1242/dev.132159

Table 2. Phenotypes of *R26(P3Cre)*$^{EnRCdx1/+}$ mice

Phenotype	% (number/total)
Ratio at birth	51.1 (71/139)
Kinked tail	47.9 (34/71)
Early postnatal death at:	
<P2	73.2 (52/71)
>P9	7.0 (5/71)
Pigmentation defects	100 (19/19)
Hydronephrosis	52.6 (10/19)

tongue and plays a major role in the control of swallowing. It is formed by several converging roots that exit the central nervous system from multiple points in the ventral part of the anterior spinal cord. In mutant embryos, these roots often appear disorganized and less dense, resulting in a reduced number of elongating axons that are also markedly shorter (Fig. 5A′-B′). Such defects are most likely due to the *P3pro-Cre*-directed expression of EnRCdx1 in the ventral region of the NT (Fig. S1D,E), and presumably reflect problems with the well-documented evolutionarily conserved role of Cdx proteins in the control of positional identity at the hindbrain-spinal cord transition via either Hox-dependent (Bel-Vialar et al., 2002; Epstein et al., 1997; Shimizu et al., 2006) or -independent (Skromne et al., 2007; Sturgeon et al., 2011) means. Regardless of the precise underlying mechanism, these hypoglossal nerve defects offer a plausible explanation for the high rate of early neonatal death in EnRCdx1 mutant offspring (Fig. 3A, Table 2).

In order to begin to understand the mechanism by which Cdx proteins impact melanocyte development, we also analyzed the expression of melanoblast markers in stage-matched control (*R26R*$^{EnRCdx1/+}$::*Cdx1*$^{-/-}$) and mutant [*R26(P3Cre)*$^{EnRCdx1/+}$::*Cdx1*$^{-/-}$] E11.5 embryos (Fig. 6). Immunofluorescence analyses for the early marker c-Kit at the level of the hindlimb buds showed that melanoblasts migrating along the dorsolateral pathway are not well aligned in the mutants (Fig. 6A,B). Intriguingly, these cells frequently appeared farther beneath the surface ectoderm and were even occasionally found to be located in dorsal root ganglia (Fig. 6B). A similar outcome was obtained with an antibody against Mitf, which in addition revealed weaker expression and abnormal cytoplasmic localization of this master transcriptional regulator of melanocyte differentiation (Fig. 6C,D). The presence of melanoblasts in ectopic locations is highly reminiscent of the phenotype observed upon NC-specific *Foxd3* loss-of-function (Nitzan et al., 2013a,b), and thus makes deficient and/or delayed cell fate decisions a likely cause of the pigmentation anomalies observed in EnRCdx1 mutants. In accordance with this, expression of the relatively late melanoblast marker *Dct* was found to be markedly reduced in the trunk region of mutant embryos, without being affected in the eye (Fig. 6E,F).

Msx1 and *Foxd3* are novel direct targets of Cdx proteins

Post-head NCCs are constantly induced at the lateral borders of the posterior neural plate (i.e. in regions containing the highest levels of Cdx proteins), concomitantly with axial elongation and the generation of new neural cells from the posterior growth zone. In an effort to identify Cdx target genes relevant to the EnRCdx1-induced NC phenotypes, we analyzed the expression of multiple markers of pre-migratory NCCs in the posterior region of E9.5 embryos via whole-mount *in situ* hybridization (Figs 7 and 8). At this stage, all three Cdx genes are robustly expressed in the tailbud region up to a varying anterior limit of weaker expression in the caudal NT. As expected from our prior work

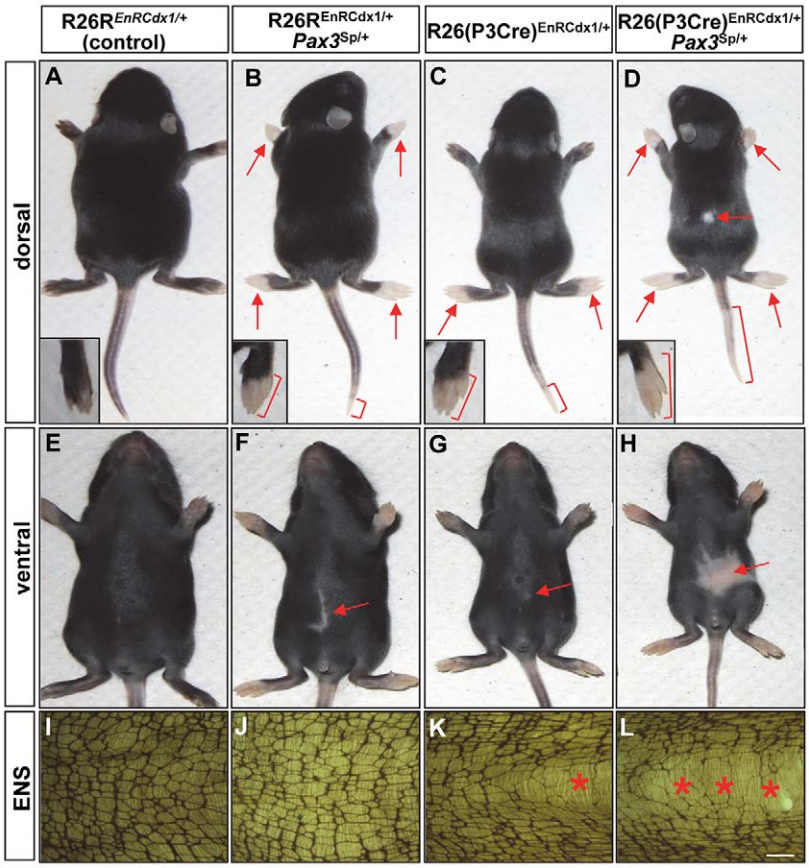

Fig. 4. Genetic interaction between *R26(P3Cre)*$^{EnRCdx1/+}$ and *Pax3*$^{Sp/+}$ animals. (A-H) Representative dorsal and ventral views of control and littermate mutants of the indicated genotypes at P10. Insets in A-D are magnified views of the left hindpaw. *R26(P3Cre)*$^{EnRCdx1/+}$ mutants (C,G) phenocopy the typical pigmentation defects (white spotting on the belly and tip of tail and paws, red arrows and brackets) of *Pax3* Splotch heterozygotes (B,F), but only at posterior levels. These posterior-specific pigmentary anomalies are considerably increased in the *Pax3*$^{Sp/+}$ background, leading to the appearance of a white spot on the back (D,H). (I-L) Staining of acetylcholinesterase activity in the myenteric plexus of the distal colonic enteric nervous system (ENS) of P30 mice. Note the presence of a small hypoganglionic patch (asterisk) in the distal colon of *R26(P3Cre)*$^{EnRCdx1/+}$ mice (K), which becomes larger in the *Pax3*$^{Sp/+}$ background (L). Scale bar: 1 mm. All images are representative of $n \geq 3$ independent observations for each genotype.

Development (2016) 143, 1363-1374 doi:10.1242/dev.132159

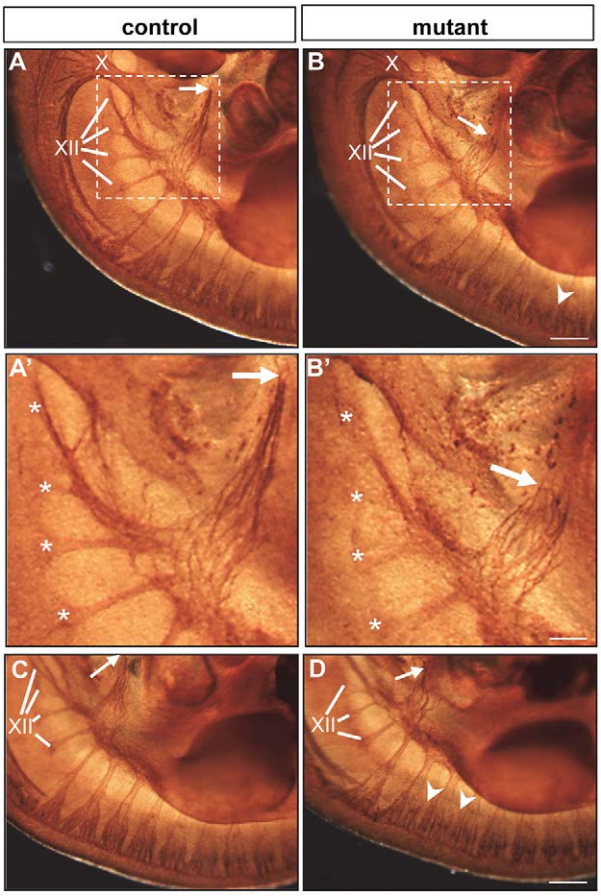

Fig. 5. Peripheral nervous system defects in *R26(P3Cre)*$^{EnRCdx1/+}$::*Cdx1*$^{-/-}$ embryos. (A-D) Whole-mount anti-neurofilament (2H3) immunohistochemistry analysis of *R26R*$^{EnRCdx1/+}$::*Cdx1*$^{-/-}$ (control) and *R26(P3Cre)*$^{EnRCdx1/+}$::*Cdx1*$^{-/-}$ (mutant) E11.5 littermate embryos. The boxed regions in A,B are magnified in A′,B′. Asterisks indicate nerve roots exiting the ventral NT. The hypoglossal nerve (XII) is less dense and markedly shorter (arrows) in mutant embryos, whereas the vagal nerve (X) is unaffected. Fusions between adjacent dorsal root ganglia are also observed (B,D, arrowheads). All images are representative of $n \geq 3$ independent observations for each genotype. Scale bars: 250 µm in A-D; 100 µm in A′,B′.

(Sanchez-Ferras et al., 2014, 2012), comparisons between stage-matched control (*R26R*$^{EnRCdx1/+}$::*Cdx1*$^{-/-}$) and mutant [*R26(P3Cre)*$^{EnRCdx1/+}$::*Cdx1*$^{-/-}$] embryos first revealed that expression of the neural plate border specifier *Pax3* is specifically reduced in pre-migratory NCCs of mutant embryos (Fig. 7A,B). Interestingly, transcript levels of the neural plate border specifier *Msx1* (Fig. 7C,D), as well as those of the NC specifier *Foxd3* (Fig. 8A,B), were also similarly reduced in mutant embryos. By contrast, expression of *Zic2*, *Sox9* and *Sox10* appeared unaffected (Fig. 7E,F, Fig. 8C-F). Importantly, all the observed EnRCdx1-mediated changes were neural specific and restricted to the caudal embryo.

To verify whether *Msx1* and *Foxd3* are novel, direct Cdx targets, we looked for relevant regulatory elements in their proximal promoter region – through which many Cdx targets are known to be regulated (Shir-Shapira et al., 2015). As Cdx proteins can regulate gene expression by either DNA binding-dependent or -independent means (Beland et al., 2004; Sanchez-Ferras et al., 2014), binding sites for Cdx as well as for Cdx-interacting proteins with a key role in NC induction were both considered to be of interest. Accordingly, analysis of the 1.2 kb proximal promoter using MatInspector software revealed consensus-like Cdx binding sites upstream of the *Foxd3* transcription start site (TSS) as well as a particular enrichment for putative Lef/Tcf binding sites upstream of both the *Msx1* and *Foxd3* TSS (Fig. 9A-C).

Luciferase assays in the NC-derived N2a cell line further showed that each Cdx member can transactivate in a dose-dependent manner both of these proximal promoters (Fig. S2). Interestingly, co-transfection of all three Cdx proteins synergistically activated the *Msx1* and *Foxd3* proximal promoters and this effect was decreased in a dose-dependent manner by $_{FLAG}$EnRCdx1 (Fig. 9D). To confirm occupancy of these loci *in vivo*, we then performed ChIP-PCR assays using trunk tissues from *R26(P3Cre)*$^{EnRCdx1/+}$::*Cdx1*$^{-/-}$ E9.5 embryos. This showed that $_{FLAG}$EnRCdx1 occupies conserved sequences containing either the consensus-like Cdx binding sites upstream of *Foxd3* or the predicted Lef/Tcf binding sites upstream of *Msx1* (Fig. 9E). These results are also in accordance with unpublished anti-Cdx2 ChIP-seq data showing peaks located at −647 bp and −823 bp from the *Msx1* and *Foxd3* TSS, respectively (D. Lohnes, personal communication). Taken together, these results demonstrate that Cdx proteins directly regulate *Msx1* and *Foxd3* expression via occupancy and transactivation of their proximal promoters.

DISCUSSION

In spite of their high, Wnt-regulated expression in the caudal neuroectoderm across chordates, the role of Cdx family members in the NC has remained obscure because of the functional redundancy, early embryonic lethality and severe posterior truncation phenotypes normally associated with the study of Cdx mutants. To circumvent these difficulties, we used a neuroectoderm-directed Cdx functional knockdown approach. This strategy resulted in posterior-restricted NC anomalies that correlated with the specific downregulation of a set of genes (*Pax3*, *Msx1* and *Foxd3*) crucial for NC specification. Our study thus confirms that a Wnt-Cdx regulatory pathway is at work during NCC ontogenesis *in vivo*.

A new potent genetic tool for the study of Cdx functions in mice

The use of an obligate repressor form of Cdx proteins *in vivo* is not new. However, in contrast to previous studies in other species that relied on EnRCdx-expressing transgenic constructs driven by different regulatory elements (Bel-Vialar et al., 2002; Isaacs et al., 1998; Katsuyama et al., 1999; Mita and Fujiwara, 2007), we generated a new *ROSA26* reporter allele (*R26R*^{EnRCdx1}), thus avoiding the problems associated with standard transgenesis (i.e. variable levels of transgene expression and/or adventitious disturbance of important endogenous sequences). Moreover, our approach not only allows the analysis of redundant Cdx functions but also greatly simplifies the study of these functions in distinct cell lineages via simple breeding with any Cre driver line of interest.

One obvious limitation of the obligate repressor approach is that any gene normally repressed by Cdx proteins will most likely remain unaffected. However, it should be noted that, in addition to the fact that Cdx-mediated repression appears to be a rare event (Verzi et al., 2011), it is also possible that the presence of the strong repressor domain of Engrailed might still lead to informative gain-of-functions in these circumstances. Another important limitation is that expression of EnRCdx1 in a Cdx-free territory might erroneously affect the expression of genes that are normally regulated by Cdx proteins in other tissues and thereby lead to biologically irrelevant interpretations. Although such potential off-

Development (2016) 143, 1363-1374 doi:10.1242/dev.132159

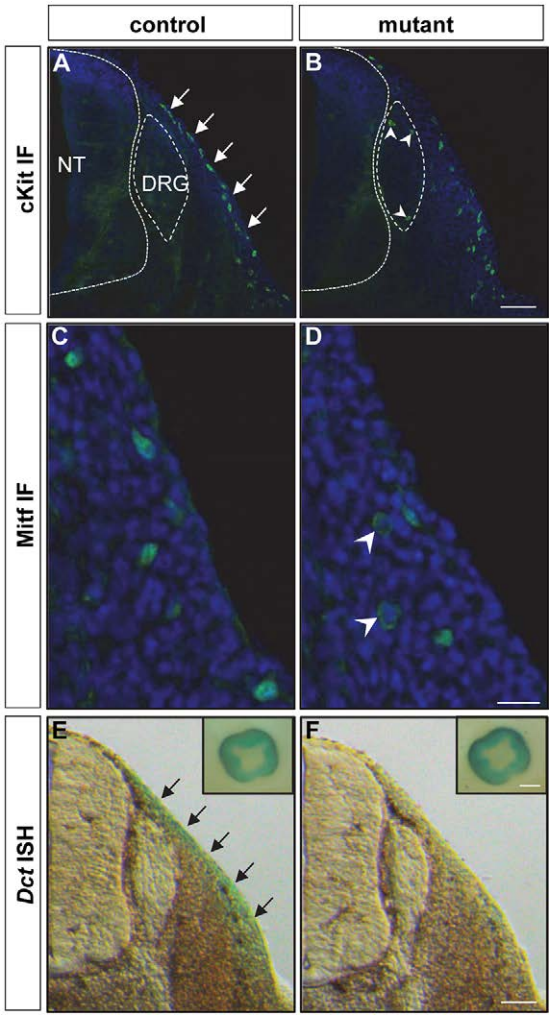

Fig. 6. Abnormal melanoblast development in *R26(P3Cre)*$^{EnRCdx1/+}$::*Cdx1*$^{-/-}$ embryos. (A-D) Immunofluorescence analyses of 40-µm transverse sections at the level of the hindlimbs in *R26R*$^{EnRCdx1/+}$::*Cdx1*$^{-/-}$ (control) and *R26(P3Cre)*$^{EnRCdx1/+}$::*Cdx1*$^{-/-}$ (mutant) E11.5 littermate embryos. (A,B) cKit^{+} melanoblasts, which are normally aligned under the surface ectoderm (A, arrows), are found in ectopic locations, such as the dorsal root ganglia (B, arrowheads), in the mutants. (C,D) Mitf expression is weaker and abnormally present in the cytoplasm (D, arrowheads) in mutant melanoblasts. (E,F) Analysis of *Dct* expression by *in situ* hybridization in *R26R*$^{EnRCdx1/+}$::*Cdx1*$^{-/-}$ (control) and *R26(P3Cre)*$^{EnRCdx1/+}$::*Cdx1*$^{-/-}$ (mutant) E11.5 littermate embryos. Vibratome transverse sections (100 µm) were cut at the level of the hindlimbs following whole-mount staining. Insets are internal positive controls showing *Dct* expression in the eye. In comparison to control embryos (E, arrows), *Dct* expression is markedly reduced under the surface ectoderm in the mutants. All images are representative of $n \geq 3$ independent observations for each genotype. Scale bars: 100 µm in A,B,E,F; 25 µm in C,D; 200 µm in insets in E,F.

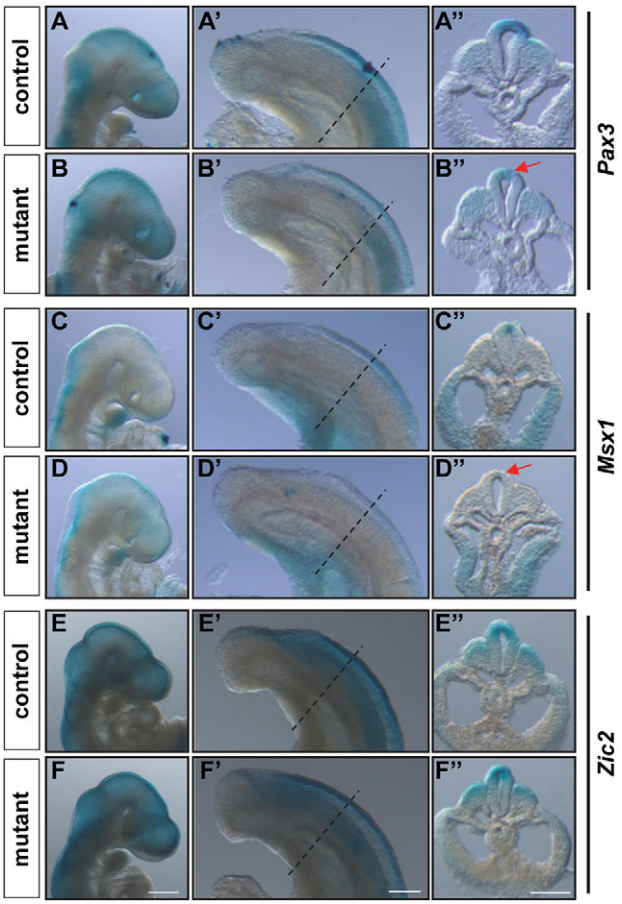

Fig. 7. Gene expression analysis of neural plate border specifiers in *R26(P3Cre)*$^{EnRCdx1/+}$::*Cdx1*$^{-/-}$ embryos. Analysis of *Pax3*, *Msx1* and *Zic2* gene expression in *R26R*$^{EnRCdx1/+}$::*Cdx1*$^{-/-}$ (control) and *R26(P3Cre)*$^{EnRCdx1/+}$::*Cdx1*$^{-/-}$ (mutant) E9.5 littermate embryos by whole-mount *in situ* hybridization. (A-F) Lateral views of the head and (A′-F′) lateral views of the tail bud region of the same embryo. Dashed lines (A′-F′) indicate the level of the transverse sections (100 µm) in A″-F″. *Pax3* and *Msx1* transcripts levels are specifically reduced in pre-migratory NCCs of mutant embryos (arrows), whereas expression of *Zic2* is unaffected. All images are representative of $n \geq 3$ independent observations for each genotype. Scale bars: 500 µm in A-F; 200 µm in A′-F″.

target effects will always remain a concern, the *P3pro-Cre* line that we used to trigger EnRCdx1 expression from the *ROSA26* locus was chosen in order to keep this risk to a minimum. Indeed, in contrast to endogenous *Pax3* expression (Goulding et al., 1991), the *P3pro-Cre* transgene is inactive in the vast majority of Cdx-free neuroectodermal tissues (anterior hindbrain, midbrain and forebrain) (Li et al., 2000; Natoli et al., 1997). It should also be noted that, although the *P3pro-Cre* transgene contains the Cdx-responsive regulatory sequences of *Pax3* (see below), the stepwise Cre-mediated expression of EnRCdx1 most likely explains why EnRCdx1 can specifically downregulate *Pax3* without affecting its own expression. Indeed, once Cre-mediated excision of the floxed interfering cassette is achieved, expression of EnRCdx1 is then permanently under the control of *ROSA26* sequences (i.e. it becomes Cre independent) and is thus no longer under the influence of Cdx proteins.

A key Cdx role at the head of the trunk NC GRN

Previous work from our group and others led us to hypothesize that, at least in the mouse, Cdx genes are at the head of the trunk NC GRN, downstream of the Wnt, FGF and BMP inductive cues. Indeed, Cdx genes are expressed in the caudal neuroectoderm before the neural plate border specifiers and are known to be regulated by these signaling pathways (Keenan et al., 2006; Lengerke et al., 2008; Pilon et al., 2006, 2007). In addition, Cdx proteins are known to mediate the regulation of canonical Wnt and BMP target genes by directly interacting with their respective nuclear effectors, namely the Lef-Tcf/β-catenin complex (Beland et al., 2004) and pSmad1/5/8 (Mari et al., 2014). Pertaining to NC development, we have specifically shown that Cdx proteins integrate canonical Wnt signaling to induce *Pax3* expression in

Development (2016) 143, 1363-1374 doi:10.1242/dev.132159

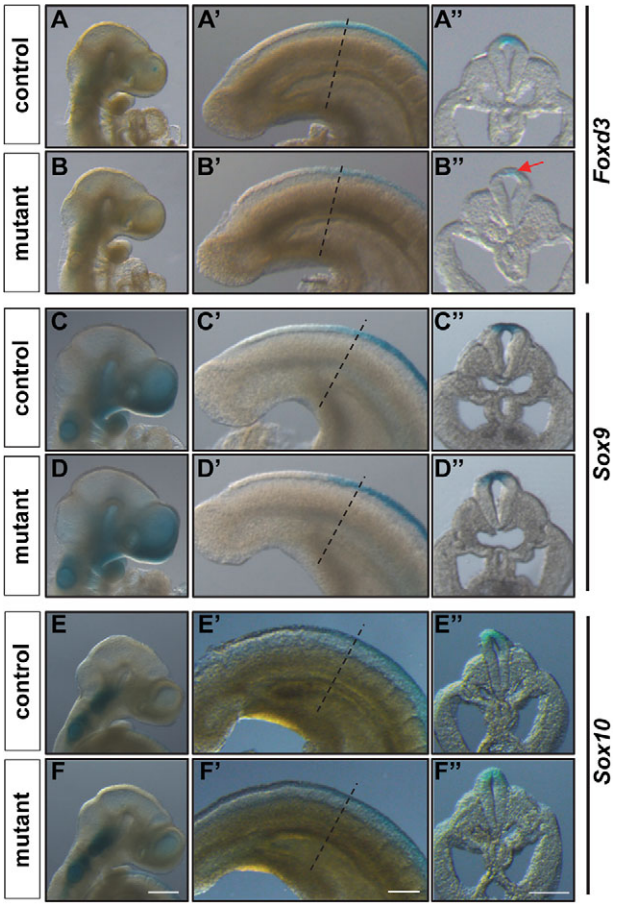

Fig. 8. Gene expression analysis of NC specifiers in *R26(P3Cre)*$^{EnRCdx1/+}$::*Cdx1*$^{-/-}$ embryos. Analysis of *Foxd3*, *Sox9* and *Sox10* gene expression in *R26R*$^{EnRCdx1/+}$::*Cdx1*$^{-/-}$ (control) and *R26(P3Cre)*$^{EnRCdx1/+}$::*Cdx1*$^{-/-}$ (mutant) E9.5 littermate embryos by whole-mount *in situ* hybridization. (A-F) Lateral views of the head and (A′-F′) lateral views of the tail bud region of the same embryo. The dashed lines (A′-F′) indicate the level of the transverse sections (100 µm) in A″-F″. *Foxd3* transcript levels are specifically reduced in pre-migratory NCCs of mutant embryos (arrow), whereas expression of *Sox9* and *Sox10* is unaffected. All images are representative of $n \geq 3$ independent observations for each genotype. Scale bars: 500 µm in A-F; 200 µm in A′-F″.

the caudal neuroectoderm by direct binding to an NC enhancer (Sanchez-Ferras et al., 2012) in association with the neural plate border specifier Zic2 (Sanchez-Ferras et al., 2014). Interestingly, both of the new Cdx targets *Msx1* and *Foxd3* (Figs 7–9) are also known to be regulated by Wnt signals during NC induction in a manner similar to *Pax3* (Taneyhill and Bronner-Fraser, 2005). This strongly suggests that the Wnt-Cdx regulatory axis can be reiteratively used to control successive overlapping steps of early trunk NC development: in specification of the posterior neural plate border via regulation of *Pax3* and *Msx1*, and in specification of the NC per se via regulation of *Foxd3*. Together with the well-known role of Cdx in the control of A-P patterning (Deschamps and van Nes, 2005; Lohnes, 2003), our work also suggests that multifunctional Cdx-dependent regulatory circuits can facilitate the coordination of NC specification with NC positional identity along the A-P axis. Such a role appears not to be restricted to the Cdx genes, since *Gbx2*, *Hoxb5* and *Meis3* – three additional A-P patterning genes – have also been reported to play important early roles in the NC GRN (Gutkovich et al., 2010; Kam et al., 2014; Li et al., 2009).

Impact of Cdx functional knockdown on melanocyte and enteric nervous system development

EnRCdx1-mediated perturbation of the NC specification program was evidenced by the presence of pigmentation and enteric nervous system abnormalities. Based on the known joint requirement of Pax3 and FoxD3 for maintaining the NC progenitor pool (Nelms et al., 2011), a likely possibility for explaining these combined defects is that the number of NCCs required for colonizing the skin and the bowel is reduced. The small hypoganglionic patch in the distal colon of *R26(P3Cre)*$^{EnRCdx1/+}$ mice and its increased size in a *Pax3*$^{Sp/+}$ background support this hypothesis (Fig. 4K,L). However, considering that the NCC defects observed upon monoallelic expression of EnRCdx1 are relatively modest, a corresponding decrease in the number of NCCs is expected to be very difficult to observe. Accordingly, our immunofluorescence analyses for the NCC marker Sox10 failed to reveal a reduction in the number of migratory NCCs in *R26(P3Cre)*$^{EnRCdx1/+}$::*Cdx1*$^{-/-}$ E9.5 embryos (Fig. S3). Of note, independently of the direct regulation of *Pax3* and *Foxd3* expression by the Cdx proteins, reduced *Msx1* expression is also expected to contribute to the NCC defects of EnRCdx1 mutants. Indeed, *Msx1* loss-of-function studies in *Xenopus* have revealed a lack of pigmentation and, interestingly, this was correlated with reduced expression of both *Pax3* and *Foxd3* (Monsoro-Burq et al., 2005). Such a role for *Msx1* in the mouse has not been reported so far, most likely because of the early perinatal lethality of *Msx1/2* single and compound mutants and the expected functional redundancy with *Msx3* (Ishii et al., 2005; Satokata and Maas, 1994; Wang et al., 1996).

Based on the relatively modest depigmentation observed in *R26(P3Cre)*$^{EnRCdx1/+}$::*Cdx1*$^{-/-}$ animals, we interpret the robust decrease of *Dct* expression that is apparent at E11.5 as a delay in the Mitf-regulated melanocyte differentiation cascade secondary to concomitant downregulation of *Pax3*, *Foxd3* and *Msx1*. Given that Mitf is known as a key direct regulator of *Dct* expression (Jiao et al., 2004; Schwahn et al., 2005), such decreased *Dct* expression is most likely due to the observed dysregulation of Mitf in mutant melanoblasts. However, the exact contribution of the combined downregulation of *Pax3*, *Foxd3* and *Msx1* to Mitf dysregulation is currently unknown. Even if we only consider the regulation of *Mitf* gene expression by Pax3, FoxD3 and Msx1, the regulatory cascade at play is expected to be complex. Indeed, Pax3, FoxD3 and Msx1 can all act as either activator or repressor depending of the molecular context, and a complex interplay is already known to exist between Pax3, FoxD3 and Mitf at both the gene and protein levels. FoxD3 can inhibit Pax3-mediated activation of *Mitf* gene expression (Thomas and Erickson, 2009) and Pax3 can inhibit activation of *Dct* expression by Mitf (Lang et al., 2005). Moreover, FoxD3 has recently been identified as a direct positive regulator of *Pax3* expression in the melanocyte lineage (Kubic et al., 2015). On the other hand, since not only the levels of Mitf but also its subcellular distribution were found to be affected in mutant melanoblasts, there is a strong possibility that supplemental, yet to be identified, Cdx targets are also involved. In this regard, it is intriguing to note that, in contrast to other cell types (Bronisz et al., 2006), actively regulated cytoplasmic-nuclear shuttling of Mitf has not been described in melanoblasts. As some Waardenburg syndrome-associated mutations of MITF (both inside and outside the nuclear localization signal) have been reported to impair its nuclear localization (Grill et al., 2013), identifying any putative Cdx target involved in the nuclear translocation of Mitf in melanoblasts might have clinical importance.

Development (2016) 143, 1363-1374 doi:10.1242/dev.132159

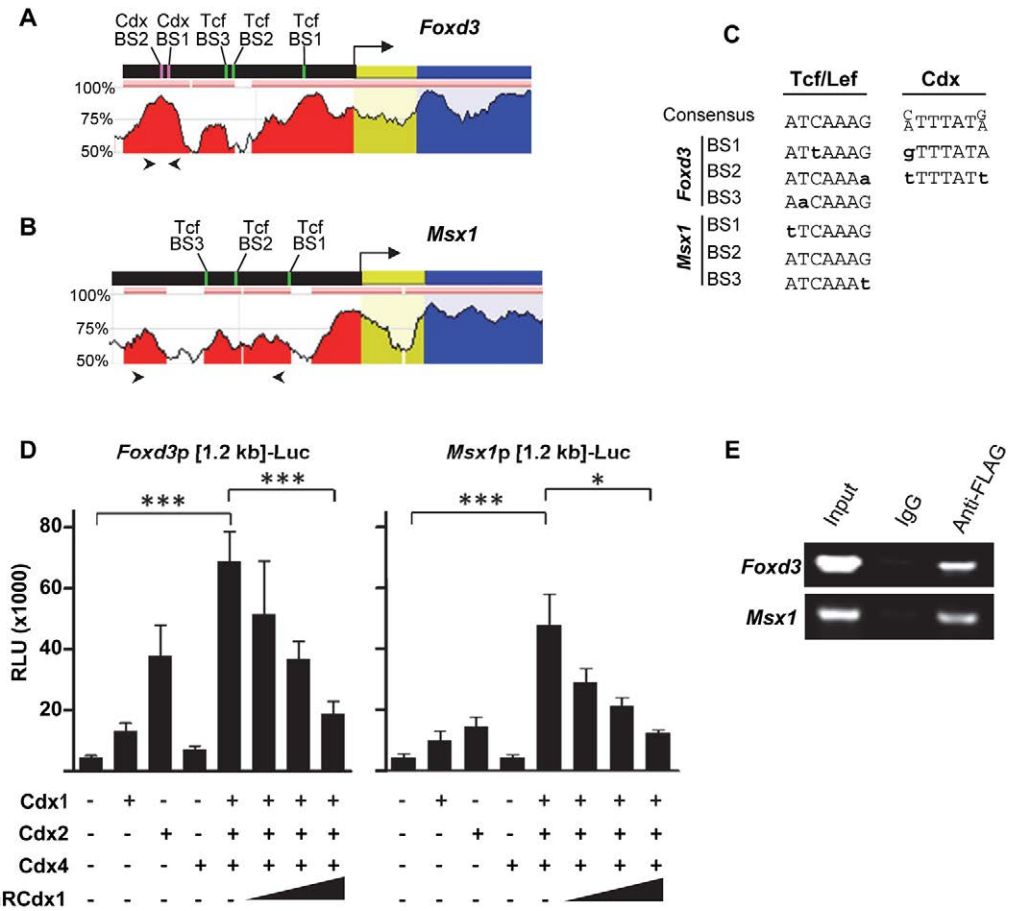

Fig. 9. Cdx proteins transactivate the proximal promoter of *Msx1* and *Foxd3*. (A,B) Comparative analysis of *Foxd3* (A) and *Msx1* (B) 5′ flanking sequences using the ECR browser (ecrbrowser.dcode.org) showing the presence of large blocks of conserved sequences (≥70% conservation between mouse and human; red peaks) within the 1.2 kb proximal promoter region of each gene. These regions are enriched in Cdx (Cdx BS) and/or Tcf/Lef (Tcf BS) binding sites. (C) Alignment of identified Cdx BS and Tcf BS with respective consensus sequences. (D) Co-transfection assays in N2a cells using luciferase reporter constructs driven by the 1.2 kb proximal promoter of *Msx1* or *Foxd3*. Results are expressed as relative luminescence units (RLU). $n \geq 5$ independent experiments performed in triplicate; error bars indicate s.e.m.; ***$P<0.001$, *$P<0.05$, one-way ANOVA and Tukey's post hoc tests. Cdx proteins transactivate each proximal promoter in a synergistic manner, an effect that is repressed by EnRCdx1 in a dose-dependent manner. (E) Anti-FLAG ChIP analysis from the trunk region of *R26(P3Cre)*$^{EnRCdx1/+}$::*Cdx1*$^{-/-}$ E9.5 embryos showing occupancy of the *Msx1* and *Foxd3* proximal promoters by $_{FLAG}$EnRCdx1 *in vivo*. The genomic position of the primers used to amplify *Foxd3* and *Msx1* conserved sequences containing Cdx BS or Tcf BS is indicated by arrowheads in A,B. These sequences are amplified from chromatin samples immunoprecipitated with anti-FLAG but not with the non-specific normal rabbit IgG control antibody. Representative images are shown of $n=3$ independent experiments.

An ancestral role for Cdx proteins in the molecular control of pigment cell development

Our work provides the first *in vivo* evidence for an indirect role of Cdx in pigment cell development in the mouse, which we believe is secondary to an early direct role in NC ontogenesis. Yet, it is noteworthy that a lack of body pigmentation has been previously reported following Cdx loss-of-function in the ascidian *Halocynthia roretzi* (Katsuyama et al., 1999). In this regard, it is also interesting that two sets of pigment cells of distinct origin have been described in ascidian embryos, and each has been suggested as the ancestral precursor of the NC (Abitua et al., 2012; Jeffery et al., 2008). One set is derived from the 'a' lineage and contributes to structures equivalent to the vertebrate eye and inner ear (Abitua et al., 2012; Nishida and Satoh, 1989), whereas the other is derived from the 'A' lineage and contributes to body pigmentation (Jeffery et al., 2008, 2004). We believe that the controversy concerning which set of pigment cells is the 'true' NC precursor could be resolved in accordance with the fact that the ascidian central nervous system is compartmentalized in a similar way to that of vertebrates (Imai et al., 2009), i.e. the origin of the cranial NC could be attributed to the a-derived set, whereas the origin of the trunk NC could be attributed to the A-derived set. The fact that ascidian Cdx is expressed in the A-line and that its inhibition results in loss of body pigmentation is in total agreement with this hypothesis (Imai et al., 2009; Katsuyama et al., 1999). Taken together with our work, these observations strongly suggest that, rather than being novel, Cdx genes might be among the most ancestral components of the trunk NC GRN.

MATERIALS AND METHODS

Ethics statement

Experiments involving mice were performed following Canadian Council of Animal Care (CCAC) guidelines for the care and manipulation of animals used in medical research. Protocols involving the manipulation of animals were approved by the Institutional Ethics Committee of the University of Quebec at Montreal [Comité Institutionnel de Protection des Animaux (CIPA)], reference number 0513-C1-648-0514.

Development (2016) 143, 1363-1374 doi:10.1242/dev.132159

Plasmid constructs

Cdx1/2/4 and $_{FLAG}$EnRCdx1 expression vectors were as previously described (Sanchez-Ferras et al., 2012) and the pMC-Cre vector was kindly provided by D. Lohnes (University of Ottawa, ON, Canada). For *in situ* hybridization probes, the *Pax3* cDNA and HA-tagged Zic2 expression vector were generous gifts from J. Epstein (University of Pennsylvania, PA, USA) and J. Aruga (RIKEN Brain Science Institute, Saitama, Japan), respectively. Plasmids containing the cDNA of *Foxd3*, *Msx1* and *Dct* were kindly provided by K. H. Kaestner (University of Pennsylvania), R. E. Maxson, Jr (University of Southern California, CA, USA) and L. Sommer (University of Zurich, Switzerland), respectively. *Sox9* and *Sox10* cDNA vectors were a kind gift from D. W. Silversides (University of Montreal, QC, Canada). The pROSA26-EnRCdx1 targeting construct was generated using the previously described pBigT and pROSA26PA vectors (Srinivas et al., 2001). *Msx1*p1.2kb-Luciferase and *Foxd3*p1.2kb-Luciferase reporter constructs were generated by subcloning respective PCR-amplified sequences (primer sequences are shown in Table S1) into pXP2 (Nordeen, 1988).

Generation of R26R-$_{FLAG}$EnRCdx1 knock-in mice

129/Sv-derived R1 ESCs were cultured as previously described (Pilon et al., 2007). These cells were electroporated with *Pvu*II-linearized pROSA26-EnRCdx1 targeting vector and selected with G418 (200 µg/ml) for 7 days. Surviving clones were isolated and analyzed for homologous recombination by Southern blot using *Eco*RI and *Kpn*I double-digested genomic DNA. Proper targeting was verified with 5′ and 3′ external probes [kindly provided by Christine Hartmann (Nyabi et al., 2009)]. Expression of the $_{FLAG}$EnRCdx1-IRES-GFP bicistronic transcript after removal of the PGKpNeo stop cassette was verified by anti-FLAG western blotting analysis and GFP fluorescence following Cre transfection (pMC-Cre) of one targeted ESC clone. This positive clone was used to generate germline chimeras by injection into C57BL/6 blastocysts according to standard procedures (Nagy et al., 2003). Mice carrying the mutant allele were identified by PCR genotyping using primers flanking the *ROSA26 Xba*I integration site (primer details are shown in Table S1).

Mice

Cdx1$^{-/-}$ mice were generously provided by D. Lohnes with the permission of P. Gruss (Subramanian et al., 1995). *Pax3*$^{+/Sp}$ and *Wnt1-Cre2* mice were obtained from the Jackson Laboratory. *T-Cre* mice were kindly provided by M. Lewandoski (Perantoni et al., 2005) and *P3pro-Cre* mice were kindly provided by S. Astrof with the permission of J. Epstein (Li et al., 2000). *P3pro-Cre*$^{Tg/+}$::*Pax3*$^{+/Sp}$ mice were generated by intercrossing *P3pro-Cre*$^{Tg/+}$ and *Pax3*$^{+/Sp}$ mice. The *P3pro-Cre*$^{Tg/+}$::*Cdx1*$^{-/-}$ and *R26R*$^{EnRCdx1/EnRCdx1}$::*Cdx1*$^{-/-}$ lines were generated by backcrossing the relevant allele into the *Cdx1*$^{-/-}$ background. *R26R*$^{EnRCdx1/+}$::*T-Cre*$^{Tg/+}$ [renamed *R26(TCre)*$^{EnRCdx1/+}$], *R26R*$^{EnRCdx1/+}$::*Wnt1-Cre2*$^{Tg/+}$ [renamed R26(W1Cre2)$^{EnRCdx1/+}$] and *R26R*$^{EnRCdx1/+}$::*P3pro-Cre*$^{Tg/+}$ [renamed *R26(P3Cre)*$^{EnRCdx1/+}$] double-heterozygous animals were generated by crossing *R26R*$^{EnRCdx1/EnRCdx1}$ mice with *T-Cre*$^{Tg/+}$, *Wnt1-Cre2*$^{Tg/+}$ and *P3pro-Cre*$^{Tg/+}$ mice, respectively. *R26R*$^{EnRCdx1/+}$::*P3pro-Cre*$^{Tg/+}$::*Cdx1*$^{-/-}$ [renamed *R26(P3Cre)*$^{EnRCdx1/+}$::*Cdx1*$^{-/-}$] animals were generated by crossing *R26R*$^{EnRCdx1/EnRCdx1}$::*Cdx1*$^{-/-}$ and *P3pro-Cre*$^{Tg/+}$::*Cdx1*$^{-/-}$ lines. *R26R*$^{EnRCdx1/+}$::*P3pro-Cre*$^{Tg/+}$::*Pax3*$^{+/Sp}$ [renamed *R26(P3Cre)*$^{EnRCdx1/+}$::*Pax3*$^{+/Sp}$] mice were generated by crossing *R26R*$^{EnRCdx1/EnRCdx1}$ mice with *P3pro-Cre*$^{Tg/+}$::*Pax3*$^{+/Sp}$ mice. All animals were on a mixed C57BL/6-129/Sv genetic background.

Offspring analysis

Embryos were generated by natural mating and collected between E9.5 and E11.5, with noon of the day of vaginal plug detection designated E0.5. Embryos to be compared were of the same litters and processed in parallel. Whole-mount *in situ* hybridization and vibratome transverse sectioning (100 µm) were performed as previously described (Coutaud and Pilon, 2013; Sanchez-Ferras et al., 2014). Skeletal preparations of newborns were performed as described (Allan et al., 2001). For acetylcholinesterase staining, the colon region from P21 control and mutant mice was dissected and stained as described (Bergeron et al., 2015).

Primary antibodies used for immunolabeling were mouse anti-neurofilament (1:200; Developmental Studies Hybridoma Bank, 2H3), goat anti-Sox10 (1:100; Santa Cruz Biotechnology, sc-17342), mouse anti-Mitf [C5] (1:2000; Abcam, ab12039) and goat anti-cKit (1:500; R&D Systems, AF1356). HRP-conjugated goat anti-mouse secondary antibody was obtained from Santa Cruz Biotechnology (sc-2005) whereas Alexa 647-conjugated bovine anti-goat and donkey anti-mouse secondary antibodies were obtained from Jackson ImmunoResearch (805-605-180 and 715-605-150). Immunohistochemistry on whole embryos and immunofluorescence on cryosections were performed as previously described (Boulende Sab et al., 2011; Sanchez-Ferras et al., 2014) except when using the anti-Mitf antibody, which required tissue permeabilization with 1% Saponin (Sigma, S-4521). Images were acquired with a Leica DFC 495 camera mounted on a Leica M205 FA microscope, except for immunofluorescence which was imaged with a Nikon A1 laser scanning confocal microscope.

Chromatin immunoprecipitation (ChIP) assays

The trunk regions from five freshly dissected E9.5 *R26(P3Cre)*$^{EnRCdx1/+}$::*Cdx1*$^{-/-}$ mouse embryos were isolated and cross-linked with 1% formaldehyde in PBS for 15 min at room temperature. ChIP assays were performed using the M-Fast Chromatin Immunoprecipitation Kit (ZmTech Scientific) in accordance with the manufacturer's instructions. Immunoprecipitation was performed as previously described (Sanchez-Ferras et al., 2014) using 1 µg mouse anti-FLAG M2 (Sigma, F1804) antibodies. Rabbit IgG was used as a negative control for immunoprecipitation. PCR amplifications were performed using Platinum Taq Hifi DNA polymerase (Invitrogen) and primers for amplifying evolutionarily conserved regions of the *Foxd3* (−1058 to −782 bp) and *Msx1* (−1137 bp to −325 bp) proximal promoters (primer details are shown in Table S1). Amplicons were resolved on a 1.5% agarose gel and confirmed by sequencing.

Transfection analysis

Transfection of Neuro2a (N2a; ATCC #CCL-131) cells and luciferase assays were performed as previously described (Sanchez-Ferras et al., 2012). For analyzing the Cdx effect on *Msx1* and *Foxd3* promoter activity, 8×10^4 N2a cells were seeded in 24-well plates and transfected with 100 ng of the respective luciferase reporter construct together with increasing amounts of Cdx1-, Cdx2- or Cdx4-IRES-GFP expression vectors (0-20 ng). For Cdx and EnRCdx1 competition assays, N2a cells were similarly transfected but with a fixed amount of Cdx1- (5 ng), Cdx2- (5 ng) and Cdx4- (10 ng) expressing vectors (alone or in combination) and increasing amounts of EnRCdx1-IRES-GFP expression vector (0-30 ng). Empty vector was included when necessary to achieve a total of 125 ng (Cdx effect) or 150 ng (EnRCdx1 competition) DNA per well. All transfections were performed at least five times in triplicate. Graphics and statistical analyses were performed with GraphPad Prism.

Acknowledgements

We thank Denis Flipo (UQAM) for FACS analyses and assistance with confocal imaging; Qinzhang Zhu [Institut de Recherches Cliniques de Montréal (IRCM)] for microinjections; and David Lohnes for sharing unpublished information regarding the Cdx2 ChIP-seq data.

Competing interests

The authors declare no competing or financial interests.

Author contributions

O.S.-F. generated the EnRCdx1 mouse, designed and performed experiments, collected and interpreted data, and wrote the manuscript. G.B. performed experiments, collected and interpreted data, and edited the manuscript. O.F., A.M.T. and O.S. performed experiments. N.P. conceived and supervised the study, and wrote the manuscript.

Funding

This work was supported by a grant from the Canadian Institutes of Health Research (CIHR) [grant number MOP-111130] to N.P.; O.S.-F. was supported by an

Alexander Graham Bell scholarship from the Natural Science and Engineering Research Council (NSERC) of Canada; and N.P. is a Fonds de la Recherche du Québec – Santé (FRQS) Junior2 scholar as well as the recipient of a UQAM Research Chair on Rare Genetic Diseases.

Supplementary information

Supplementary information available online at
http://dev.biologists.org/lookup/suppl/doi:10.1242/dev.132159/-/DC1

References

Abitua, P. B., Wagner, E., Navarrete, I. A. and Levine, M. (2012). Identification of a rudimentary neural crest in a non-vertebrate chordate. *Nature* **492**, 104-107.
Allan, D., Houle, M., Bouchard, N., Meyer, B. I., Gruss, P. and Lohnes, D. (2001). RARgamma and Cdx1 interactions in vertebral patterning. *Dev. Biol.* **240**, 46-60.
Bansal, D., Scholl, C., Frohling, S., McDowell, E., Lee, B. H., Dohner, K., Ernst, P., Davidson, A. J., Daley, G. Q., Zon, L. I. et al. (2006). Cdx4 dysregulates Hox gene expression and generates acute myeloid leukemia alone and in cooperation with Meis1a in a murine model. *Proc. Natl. Acad. Sci. USA* **103**, 16924-16929.
Barriga, E. H., Trainor, P. A., Bronner, M. and Mayor, R. (2015). Animal models for studying neural crest development: is the mouse different? *Development* **142**, 1555-1560.
Beck, F., Erler, T., Russell, A. and James, R. (1995). Expression of Cdx-2 in the mouse embryo and placenta: possible role in patterning of the extra-embryonic membranes. *Dev. Dyn.* **204**, 219-227.
Beland, M., Pilon, N., Houle, M., Oh, K., Sylvestre, J.-R., Prinos, P. and Lohnes, D. (2004). Cdx1 autoregulation is governed by a novel Cdx1-LEF1 transcription complex. *Mol. Cell. Biol.* **24**, 5028-5038.
Bel-Vialar, S., Itasaki, N. and Krumlauf, R. (2002). Initiating Hox gene expression: in the early chick neural tube differential sensitivity to FGF and RA signaling subdivides the HoxB genes in two distinct groups. *Development* **129**, 5103-5115.
Bergeron, K.-F., Cardinal, T., Touré, A. M., Beland, M., Raiwet, D. L., Silversides, D. W. and Pilon, N. (2015). Male-biased aganglionic megacolon in the TashT mouse line due to perturbation of silencer elements in a large gene desert of chromosome 10. *PLoS Genet.* **11**, e1005093.
Boulende Sab, A., Bouchard, M.-F., Béland, M., Prud'homme, B., Souchkova, O., Viger, R. S. and Pilon, N. (2011). An Ebox element in the proximal Gata4 promoter is required for Gata4 expression in vivo. *PLoS ONE* **6**, e29038.
Bronisz, A., Sharma, S. M., Hu, R., Godlewski, J., Tzivion, G., Mansky, K. C. and Ostrowski, M. C. (2006). Microphthalmia-associated transcription factor interactions with 14-3-3 modulate differentiation of committed myeloid precursors. *Mol. Biol. Cell* **17**, 3897-3906.
Bronner, M. E. and LeDouarin, N. M. (2012). Development and evolution of the neural crest: an overview. *Dev. Biol.* **366**, 2-9.
Copf, T., Schroder, R. and Averof, M. (2004). Ancestral role of caudal genes in axis elongation and segmentation. *Proc. Natl. Acad. Sci. USA* **101**, 17711-17715.
Coutaud, B. and Pilon, N. (2013). Characterization of a novel transgenic mouse line expressing Cre recombinase under the control of the Cdx2 neural specific enhancer. *Genesis* **51**, 777-784.
Deschamps, J. and van Nes, J. (2005). Developmental regulation of the Hox genes during axial morphogenesis in the mouse. *Development* **132**, 2931-2942.
Epstein, M., Pillemer, G., Yelin, R., Yisraeli, J. K. and Fainsod, A. (1997). Patterning of the embryo along the anterior-posterior axis: the role of the caudal genes. *Development* **124**, 3805-3814.
Faas, L. and Isaacs, H. V. (2009). Overlapping functions of Cdx1, Cdx2, and Cdx4 in the development of the amphibian Xenopus tropicalis. *Dev. Dyn.* **238**, 835-852.
Gamer, L. W. and Wright, C. V. (1993). Murine Cdx-4 bears striking similarities to the Drosophila caudal gene in its homeodomain sequence and early expression pattern. *Mech. Dev.* **43**, 71-81.
Gaunt, S. J., Drage, D. and Cockley, A. (2003). Vertebrate caudal gene expression gradients investigated by use of chick cdx-A/lacZ and mouse cdx-1/lacZ reporters in transgenic mouse embryos: evidence for an intron enhancer. *Mech. Dev.* **120**, 573-586.
Gaunt, S. J., Drage, D. and Trubshaw, R. C. (2005). cdx4/lacZ and cdx2/lacZ protein gradients formed by decay during gastrulation in the mouse. *Int. J. Dev. Biol.* **49**, 901-908.
Goulding, M. D., Chalepakis, G., Deutsch, U., Erselius, J. R. and Gruss, P. (1991). Pax-3, a novel murine DNA binding protein expressed during early neurogenesis. *EMBO J.* **10**, 1135-1147.
Green, S. A. and Bronner, M. E. (2013). Gene duplications and the early evolution of neural crest development. *Semin. Cell Dev. Biol.* **24**, 95-100.
Grill, C., Bergsteinsdottir, K., Ogmundsdottir, M. H., Pogenberg, V., Schepsky, A., Wilmanns, M., Pingault, V. and Steingrimsson, E. (2013). MITF mutations associated with pigment deficiency syndromes and melanoma have different effects on protein function. *Hum. Mol. Genet.* **22**, 4357-4367.
Gutkovich, Y. E., Ofir, R., Elkouby, Y. M., Dibner, C., Gefen, A., Elias, S. and Frank, D. (2010). Xenopus Meis3 protein lies at a nexus downstream to Zic1 and Pax3 proteins, regulating multiple cell-fates during early nervous system development. *Dev. Biol.* **338**, 50-62.
Imai, K. S., Stolfi, A., Levine, M. and Satou, Y. (2009). Gene regulatory networks underlying the compartmentalization of the Ciona central nervous system. *Development* **136**, 285-293.
Isaacs, H. V., Pownall, M. E. and Slack, J. M. W. (1998). Regulation of Hox gene expression and posterior development by the Xenopus caudal homologue Xcad3. *EMBO J.* **17**, 3413-3427.
Ishii, M., Han, J., Yen, H.-Y., Sucov, H. M., Chai, Y. and Maxson, R. E., Jr. (2005). Combined deficiencies of Msx1 and Msx2 cause impaired patterning and survival of the cranial neural crest. *Development* **132**, 4937-4950.
Jeffery, W. R., Strickler, A. G. and Yamamoto, Y. (2004). Migratory neural crest-like cells form body pigmentation in a urochordate embryo. *Nature* **431**, 696-699.
Jeffery, W. R., Chiba, T., Krajka, F. R., Deyts, C., Satoh, N. and Joly, J.-S. (2008). Trunk lateral cells are neural crest-like cells in the ascidian Ciona intestinalis: insights into the ancestry and evolution of the neural crest. *Dev. Biol.* **324**, 152-160.
Jiao, Z., Mollaaghababa, R., Pavan, W. J., Antonellis, A., Green, E. D. and Hornyak, T. J. (2004). Direct interaction of Sox10 with the promoter of murine Dopachrome Tautomerase (Dct) and synergistic activation of Dct expression with Mitf. *Pigment Cell Res.* **17**, 352-362.
Kam, M. K. M., Cheung, M., Zhu, J. J., Cheng, W. W. C., Sat, E. W., Tam, P. K. H. and Lui, V. C. H. (2014). Homeobox b5 (Hoxb5) regulates the expression of Forkhead box D3 gene (Foxd3) in neural crest. *Int. J. Biochem. Cell Biol.* **55**, 144-152.
Katsuyama, Y., Sato, Y., Wada, S. and Saiga, H. (1999). Ascidian tail formation requires caudal function. *Dev. Biol.* **213**, 257-268.
Keenan, I. D., Sharrard, R. M. and Isaacs, H. V. (2006). FGF signal transduction and the regulation of Cdx gene expression. *Dev. Biol.* **299**, 478-488.
Kubic, J. D., Little, E. C., Kaiser, R. S., Young, K. P. and Lang, D. (2015). FOXD3 promotes PAX3 expression in melanoma cells. *J. Cell. Biochem.* **117**, 533-541.
Kuo, B. R. and Erickson, C. A. (2010). Regional differences in neural crest morphogenesis. *Cell Adhes. Migr.* **4**, 567-585.
Lang, D., Chen, F., Milewski, R., Li, J., Lu, M. M. and Epstein, J. A. (2000). Pax3 is required for enteric ganglia formation and functions with Sox10 to modulate expression of c-ret. *J. Clin. Invest.* **106**, 963-971.
Lang, D., Lu, M. M., Huang, L., Engleka, K. A., Zhang, M., Chu, E. Y., Lipner, S., Skoultchi, A., Millar, S. E. and Epstein, J. A. (2005). Pax3 functions at a nodal point in melanocyte stem cell differentiation. *Nature* **433**, 884-887.
Lengerke, C., Schmitt, S., Bowman, T. V., Jang, I. H., Maouche-Chretien, L., McKinney-Freeman, S., Davidson, A. J., Hammerschmidt, M., Rentzsch, F., Green, J. B. et al. (2008). BMP and Wnt specify hematopoietic fate by activation of the Cdx-Hox pathway. *Cell Stem Cell* **2**, 72-82.
Li, J., Chen, F. and Epstein, J. A. (2000). Neural crest expression of Cre recombinase directed by the proximal Pax3 promoter in transgenic mice. *Genesis* **26**, 162-164.
Li, B., Kuriyama, S., Moreno, M. and Mayor, R. (2009). The posteriorizing gene Gbx2 is a direct target of Wnt signalling and the earliest factor in neural crest induction. *Development* **136**, 3267-3278.
Lickert, H., Domon, C., Huls, G., Wehrle, C., Duluc, I., Clevers, H., Meyer, B. I., Freund, J. N. and Kemler, R. (2000). Wnt/(beta)-catenin signaling regulates the expression of the homeobox gene Cdx1 in embryonic intestine. *Development* **127**, 3805-3813.
Liu, S., Liu, F., Schneider, A. E., St. Amand, T., Epstein, J. A. and Gutstein, D. E. (2006). Distinct cardiac malformations caused by absence of connexin 43 in the neural crest and in the non-crest neural tube. *Development* **133**, 2063-2073.
Lohnes, D. (2003). The Cdx1 homeodomain protein: an integrator of posterior signaling in the mouse. *Bioessays* **25**, 971-980.
Mari, L., Milano, F., Parikh, K., Straub, D., Everts, V., Hoeben, K. K., Fockens, P., Buttar, N. S. and Krishnadath, K. K. (2014). A pSMAD/CDX2 complex is essential for the intestinalization of epithelial metaplasia. *Cell Rep.* **7**, 1197-1210.
Meyer, B. I. and Gruss, P. (1993). Mouse Cdx-1 expression during gastrulation. *Development* **117**, 191-203.
Mita, K. and Fujiwara, S. (2007). Nodal regulates neural tube formation in the Ciona intestinalis embryo. *Dev. Genes Evol.* **217**, 593-601.
Monsoro-Burq, A.-H., Wang, E. and Harland, R. (2005). Msx1 and Pax3 cooperate to mediate FGF8 and WNT signals during Xenopus neural crest induction. *Dev. Cell* **8**, 167-178.
Nagy, A., Gertsenstein, M., Vintersten, K. and Behringer, R. (2003). *Manipulating the Mouse Embryo, A Laboratory Manual*, 3rd edn. Cold spring Harbor, New York: Cold Spring Harbor Laboratory Press.
Natoli, T. A., Ellsworth, M. K., Wu, C., Gross, K. W. and Pruitt, S. C. (1997). Positive and negative DNA sequence elements are required to establish the pattern of Pax3 expression. *Development* **124**, 617-626.
Nelms, B. L., Pfaltzgraff, E. R. and Labosky, P. A. (2011). Functional interaction between Foxd3 and Pax3 in cardiac neural crest development. *Genesis* **49**, 10-23.
Nishida, H. and Satoh, N. (1989). Determination and regulation in the pigment cell lineage of the ascidian embryo. *Dev. Biol.* **132**, 355-367.
Nitzan, E., Krispin, S., Pfaltzgraff, E. R., Klar, A., Labosky, P. A. and Kalcheim, C. (2013a). A dynamic code of dorsal neural tube genes regulates the segregation between neurogenic and melanogenic neural crest cells. *Development* **140**, 2269-2279.

Development (2016) 143, 1363-1374 doi:10.1242/dev.132159

Nitzan, E., Pfaltzgraff, E. R., Labosky, P. A. and Kalcheim, C. (2013b). Neural crest and Schwann cell progenitor-derived melanocytes are two spatially segregated populations similarly regulated by Foxd3. *Proc. Natl. Acad. Sci. USA* **110**, 12709-12714.

Nordeen, S. K. (1988). Luciferase reporter gene vectors for analysis of promoters and enhancers. *Biotechniques* **6**, 454-458.

Nyabi, O., Naessens, M., Haigh, K., Gembarska, A., Goossens, S., Maetens, M., De Clercq, S., Drogat, B., Haenebalcke, L., Bartunkova, S. et al. (2009). Efficient mouse transgenesis using Gateway-compatible ROSA26 locus targeting vectors and F1 hybrid ES cells. *Nucleic Acids Res.* **37**, e55.

Perantoni, A. O., Timofeeva, O., Naillat, F., Richman, C., Pajni-Underwood, S., Wilson, C., Vainio, S., Dove, L. F. and Lewandoski, M. (2005). Inactivation of FGF8 in early mesoderm reveals an essential role in kidney development. *Development* **132**, 3859-3871.

Pilon, N., Oh, K., Sylvestre, J.-R., Bouchard, N., Savory, J. and Lohnes, D. (2006). Cdx4 is a direct target of the canonical Wnt pathway. *Dev. Biol.* **289**, 55-63.

Pilon, N., Oh, K., Sylvestre, J.-R., Savory, J. G. A. and Lohnes, D. (2007). Wnt signaling is a key mediator of Cdx1 expression in vivo. *Development* **134**, 2315-2323.

Prinos, P., Joseph, S., Oh, K., Meyer, B. I., Gruss, P. and Lohnes, D. (2001). Multiple pathways governing Cdx1 expression during murine development. *Dev. Biol.* **239**, 257-269.

Sanchez-Ferras, O., Coutaud, B., Djavanbakht Samani, T., Tremblay, I., Souchkova, O. and Pilon, N. (2012). Caudal-related homeobox (Cdx) protein-dependent integration of canonical Wnt signaling on paired-box 3 (Pax3) neural crest enhancer. *J. Biol. Chem.* **287**, 16623-16635.

Sanchez-Ferras, O., Bernas, G., Laberge-Perrault, E. and Pilon, N. (2014). Induction and dorsal restriction of Paired-box 3 (Pax3) gene expression in the caudal neuroectoderm is mediated by integration of multiple pathways on a short neural crest enhancer. *Biochim. Biophys. Acta* **1839**, 546-558.

Satokata, I. and Maas, R. (1994). Msx1 deficient mice exhibit cleft palate and abnormalities of craniofacial and tooth development. *Nat. Genet.* **6**, 348-356.

Savory, J. G. A., Bouchard, N., Pierre, V., Rijli, F. M., De Repentigny, Y., Kothary, R. and Lohnes, D. (2009a). Cdx2 regulation of posterior development through non-Hox targets. *Development* **136**, 4099-4110.

Savory, J. G. A., Pilon, N., Grainger, S., Sylvestre, J.-R., Béland, M., Houle, M., Oh, K. and Lohnes, D. (2009b). Cdx1 and Cdx2 are functionally equivalent in vertebral patterning. *Dev. Biol.* **330**, 114-122.

Savory, J. G. A., Mansfield, M., Rijli, F. M. and Lohnes, D. (2011). Cdx mediates neural tube closure through transcriptional regulation of the planar cell polarity gene Ptk7. *Development* **138**, 1361-1370.

Schwahn, D. J., Timchenko, N. A., Shibahara, S. and Medrano, E. E. (2005). Dynamic regulation of the human dopachrome tautomerase promoter by MITF, ER-alpha and chromatin remodelers during proliferation and senescence of human melanocytes. *Pigment Cell Res.* **18**, 203-213.

Shimizu, T., Bae, Y.-K., Muraoka, O. and Hibi, M. (2005). Interaction of Wnt and caudal-related genes in zebrafish posterior body formation. *Dev. Biol.* **279**, 125-141.

Shimizu, T., Bae, Y.-K. and Hibi, M. (2006). Cdx-Hox code controls competence for responding to Fgfs and retinoic acid in zebrafish neural tissue. *Development* **133**, 4709-4719.

Shinmyo, Y., Mito, T., Matsushita, T., Sarashina, I., Miyawaki, K., Ohuchi, H. and Noji, S. (2005). caudal is required for gnathal and thoracic patterning and for posterior elongation in the intermediate-germband cricket Gryllus bimaculatus. *Mech. Dev.* **122**, 231-239.

Shir-Shapira, H., Sharabany, J., Filderman, M., Ideses, D., Ovadia-Shochat, A., Mannervik, M. and Juven-Gershon, T. (2015). Structure-function analysis of the drosophila melanogaster caudal transcription factor provides insights into core promoter-preferential activation. *J. Biol. Chem.* **290**, 17293-17305.

Simoes-Costa, M. and Bronner, M. E. (2013). Insights into neural crest development and evolution from genomic analysis. *Genome Res.* **23**, 1069-1080.

Simoes-Costa, M. and Bronner, M. E. (2015). Establishing neural crest identity: a gene regulatory recipe. *Development* **142**, 242-257.

Skromne, I., Thorsen, D., Hale, M., Prince, V. E. and Ho, R. K. (2007). Repression of the hindbrain developmental program by Cdx factors is required for the specification of the vertebrate spinal cord. *Development* **134**, 2147-2158.

Srinivas, S., Watanabe, T., Lin, C.-S., William, C. M., Tanabe, Y., Jessell, T. M. and Costantini, F. (2001). Cre reporter strains produced by targeted insertion of EYFP and ECFP into the ROSA26 locus. *BMC Dev. Biol.* **1**, 4.

Stottmann, R. W. and Klingensmith, J. (2011). Bone morphogenetic protein signaling is required in the dorsal neural folds before neurulation for the induction of spinal neural crest cells and dorsal neurons. *Dev. Dyn.* **240**, 755-765.

Stuhlmiller, T. J. and García-Castro, M. I. (2012). Current perspectives of the signaling pathways directing neural crest induction. *Cell. Mol. Life Sci.* **69**, 3715-3737.

Sturgeon, K., Kaneko, T., Biemann, M., Gauthier, A., Chawengsaksophak, K. and Cordes, S. P. (2011). Cdx1 refines positional identity of the vertebrate hindbrain by directly repressing Mafb expression. *Development* **138**, 65-74.

Subramanian, V., Meyer, B. I. and Gruss, P. (1995). Disruption of the murine homeobox gene Cdx1 affects axial skeletal identities by altering the mesodermal expression domains of Hox genes. *Cell* **83**, 641-653.

Taneyhill, L. A. and Bronner-Fraser, M. (2005). Dynamic alterations in gene expression after Wnt-mediated induction of avian neural crest. *Mol. Biol. Cell* **16**, 5283-5293.

Taylor, J. K., Levy, T., Suh, E. R. and Traber, P. G. (1997). Activation of enhancer elements by the homeobox gene Cdx2 is cell line specific. *Nucleic Acids Res.* **25**, 2293-2300.

Thomas, A. J. and Erickson, C. A. (2009). FOXD3 regulates the lineage switch between neural crest-derived glial cells and pigment cells by repressing MITF through a non-canonical mechanism. *Development* **136**, 1849-1858.

Turgeon, B. and Meloche, S. (2009). Interpreting neonatal lethal phenotypes in mouse mutants: insights into gene function and human diseases. *Physiol. Rev.* **89**, 1-26.

van den Akker, E., Forlani, S., Chawengsaksophak, K., de Graaff, W., Beck, F., Meyer, B. I. and Deschamps, J. (2002). Cdx1 and Cdx2 have overlapping functions in anteroposterior patterning and posterior axis elongation. *Development* **129**, 2181-2193.

van Nes, J., de Graaff, W., Lebrin, F., Gerhard, M., Beck, F. and Deschamps, J. (2006). The Cdx4 mutation affects axial development and reveals an essential role of Cdx genes in the ontogenesis of the placental labyrinth in mice. *Development* **133**, 419-428.

van Rooijen, C., Simmini, S., Bialecka, M., Neijts, R., van de Ven, C., Beck, F. and Deschamps, J. (2012). Evolutionarily conserved requirement of Cdx for post-occipital tissue emergence. *Development* **139**, 2576-2583.

Verzi, M. P., Shin, H., Ho, L.-L., Liu, X. S. and Shivdasani, R. A. (2011). Essential and redundant functions of caudal family proteins in activating adult intestinal genes. *Mol. Cell. Biol.* **31**, 2026-2039.

Wang, W., Chen, X., Xu, H. and Lufkin, T. (1996). Msx3: a novel murine homologue of the Drosophila msh homeog gene restricted to the dorsal embryonic central nervous system. *Mech. Dev.* **58**, 203-215.

Young, T., Rowland, J. E., van de Ven, C., Bialecka, M., Novoa, A., Carapuco, M., van Nes, J., de Graaff, W., Duluc, I., Freund, J.-N. et al. (2009). Cdx and Hox genes differentially regulate posterior axial growth in mammalian embryos. *Dev. Cell* **17**, 516-526.

Zhao, T., Gan, Q., Stokes, A., Lassiter, R. N. T., Wang, Y., Chan, J., Han, J. X., Pleasure, D. E., Epstein, J. A. and Zhou, C. J. (2014). beta-catenin regulates Pax3 and Cdx2 for caudal neural tube closure and elongation. *Development* **141**, 148-157.

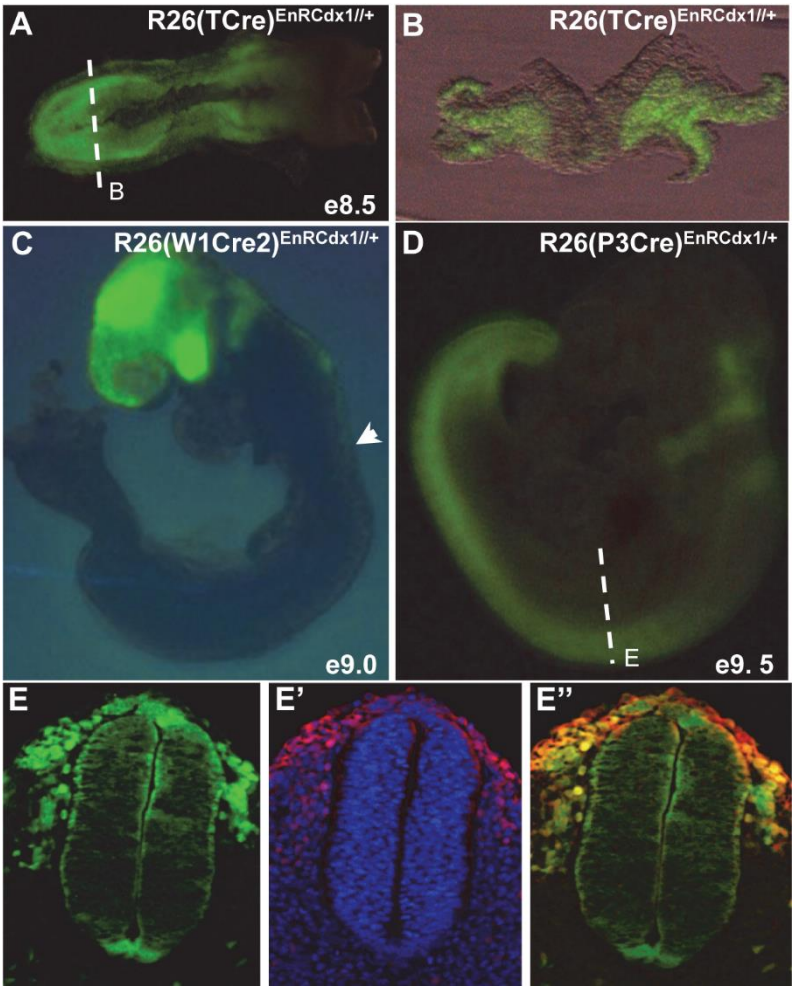

Figure S1. Validation of Cre-mediated expression of the EnRCdx1-IRES-GFP bicistronic transcript in embryos.

(A-B) GFP fluorescence in an e8.5 R26(TCre)$^{EnRCdx1/+}$embryo (dorsal view) showing expression in the posterior nascent mesoderm and derivatives. The dashed line in A indicates the level at which the transverse section shown in B was made. **(C)** GFP fluorescence in an e9.0 R26(W1Cre2)$^{EnRCdx1/+}$ embryo (lateral view) showing expression in the craniofacial region as well as in the dorsal NT with a posterior limit in the anterior spinal cord territory (arrowhead). **(D)** GFP fluorescence in an e9.5 R26(P3Cre)$^{EnRCdx1/+}$ embryo (lateral view) showing expression in the whole posterior neuroectoderm with an anterior limit in the posterior hindbrain. The dashed line indicates the level at which the section shown in E was made. **(E-E")** Endogenous GFP fluorescence (E) and anti-Sox10 immunofluorescence (E') in a vibratome transverse section (100 µm) at the level of the forelimb bud of a R26(P3Cre)$^{EnRCdx1/+}$ embryo showing coexpression of GFP and Sox10 in NCC (E").

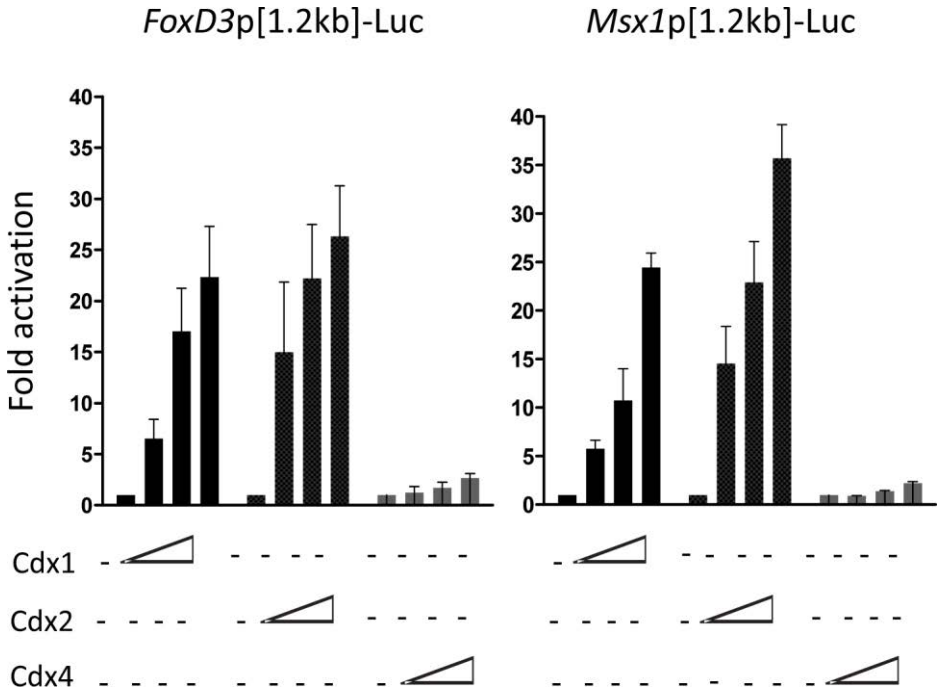

Figure S2. Cdx1, Cdx2 and Cdx4 differentially transactivate the proximal promoter of *Msx1* and *FoxD3*.

Co-transfection assays in N2a cells using luciferase reporter constructs driven by the 1.2 kb proximal promoter of *Msx1* and *FoxD3* as well as Cdx1, Cdx2, Cdx4 expression vectors. The results are expressed as fold induction compared to the relevant reporter vector alone (n=5 independent experiments performed in triplicate; error bars indicate s.e.m.). Note that addition of Cdx1, Cdx2 or Cdx4 expression constructs transactivates *Msx1* and *FoxD3* promoter sequences in a dose-dependent manner. Note also that Cdx proteins exhibit differential transcriptional activity, with Cdx2 eliciting the strongest response, followed by Cdx1 and then by Cdx4.

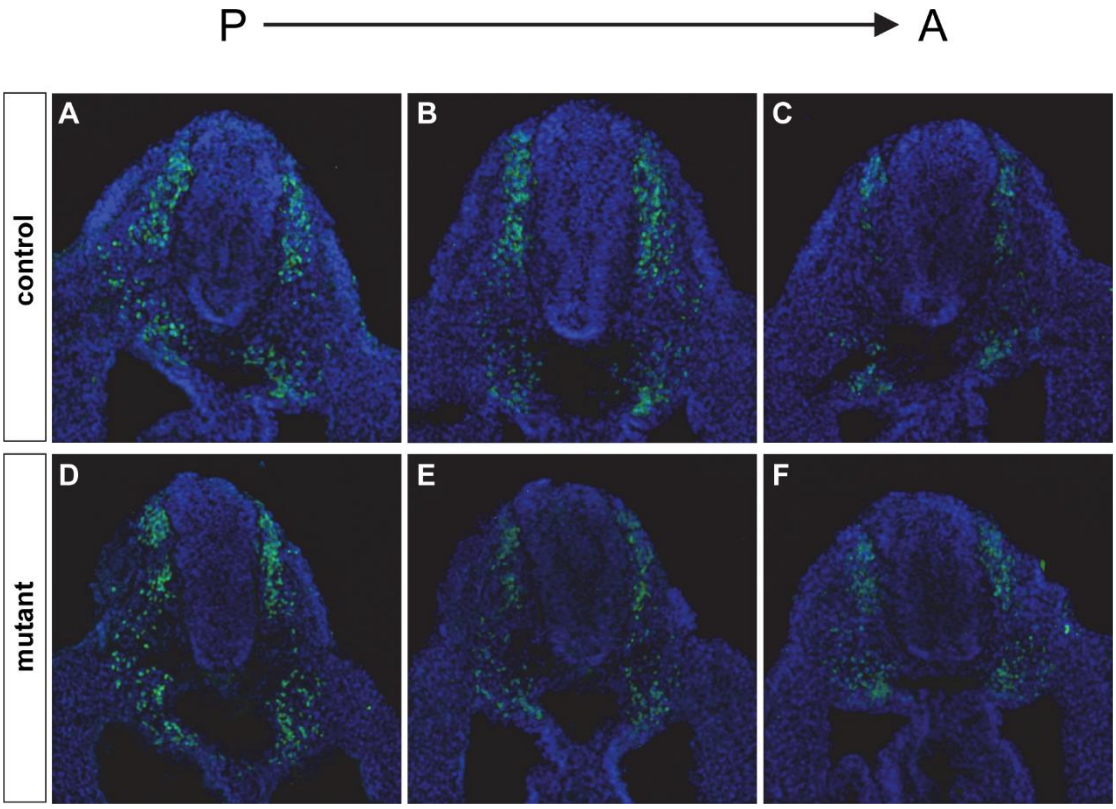

Figure S3. The number of Sox10^{+} migratory NCC appears unaffected in R26(P3Cre)$^{EnRCdx1/+}$::*Cdx1*$^{-/-}$ e9.5 embryos.

(A-F) Anti-Sox10 immunofluorescence analysis of 40µm transverse sections taken from the trunk of R26R$^{EnRCdx1/+}$::*Cdx1*$^{-/-}$ (control) and R26(P3Cre)$^{EnRCdx1/+}$::*Cdx1*$^{-/-}$ (mutant) e9.5 littermate embryos. No obvious difference in the number of NCC is noted between mutants and controls. P, posterior; A, anterior.

Table S1. List of oligonucleotides used in this study.

Primer name	**sequence 5' to 3'**
Msx1 1.2kb promoter Forward	gga tcc cgg cag tca tca atg cac ag
Msx1 1.2kb promoter Reverse	ctc gag gtt aat aag gca agg cca gc
Foxd3 1.2kb promoter Forward	gga tcc ctc cac tcg gaa gta tac gc
Foxd3 1.2kb promoter Reverse	ctc gag ggt ttg ggc gtg ggg ttc ag
Foxd3 ChIP Forward	ctc cgt ttc cag ctc att tcc gac
Foxd3 ChIP Reverse	ctc aag tct tac cct agc ttt ccg
Msx1 ChIP Forward	ctc ccc aac agc ctg ttc gaa c
Msx1 ChIP Reverse	ccc act tct tct gtt cct ctc c
ROSA26R genotyping Forward	ccc aaa gtc gct ctg agt tgt tat c
ROSA26R genotyping Reverse	tgc gcc cta cag atc cct taa tta a
ROSA26WT genotyping Reverse	cca gat gac tac cta tcc tcc ca